

**INDIAN OCEAN SKIPJACK TUNA STOCK ASSESSMENT 1950-2022
(STOCK SYNTHESIS)**

PREPARED BY: DAN FU¹,

20 OCTOBER 2023

¹ IOTC Secretariat, Dan.Fu@fao.org;

Contents

1. INTRODUCTION.....	4
1.1 Biology and stock structure.....	4
1.2 Fishery overview.....	5
2. OBSERVATIONS AND MODEL INPUTS.....	6
2.1 Spatial stratification	7
2.2 Temporal stratification.....	7
2.3 Definition of fisheries	7
2.4 Catch history	8
2.5 CPUE indices.....	8
2.5.1 Maldives PL CPUE series.....	8
2.5.2 EUROPEAN PSLs abundance indices series.....	8
2.5.3 Other abundance indices	8
2.6 Length frequency data.....	9
2.7 Tagging data.....	10
3. Model structural and assumptions	14
3.1 Population dynamics	14
3.1.1 Recruitment.....	14
3.1.2 Growth and Maturation.....	14
3.1.3 Natural mortality	15
3.2 Fishery dynamics	15
3.3 Dynamics of tagged fish	16
3.4 Modelling methods, parameters, and likelihood.....	16
3.5 Reference points.....	17
4. ASSESSMENT model runs.....	17
4.1 2020 model continuity run	17
4.2 Basic and sensitivity models	18
4.3 Proposed model ensemble (grid).....	20
5. model RESULTS.....	21
5.1 2020 model continuity run	21
5.2 Basic models	21
5.2.1 Model fits.....	21
5.2.2 Model estimates	29
5.3 Sensitivity models.....	32
5.4 Proposed model ensemble.....	33
5.5 Diagnostics.....	36
5.5.1 Jitter analysing	36
5.5.2 Profile likelihood.....	37
5.5.3 Retrospective analysis.....	38
6. Stock status.....	39
6.1 Current status and yields.....	39
7. DISCUSSION	42
8. ACKNOWLEDGMENTS	44
9. REFERENCES.....	44
Appendix A: SELECTED RESULTS FROM THE SENSIVITY MODELS.....	48

SUMMARY

This report summarises a stock assessment for Indian Ocean Skipjack tuna (*Katsuwona pelamis*) using *Stock Synthesis 3* (SS3). The assessment assumed the Indian Ocean skipjack tuna constitute a single stock and is based on a spatially aggregated and seasonally structured model that integrates several sources of fisheries and biological data. The assessment model covers the period 1950–2022 and represents an update and revision of the 2020 assessment model with the inclusion of updated CPUE indices and length composition data. Standardised CPUE series from Maldives Pole and line fleet 1995 – 2022 and EU associated Purse seine sets 1990 – 2021 were included in the models as relative abundance index of exploitable biomass. An additional index based on associative dynamics of skipjack tuna with floating objects was considered as an alternative index for the abundance trend for more recent years (2013–2022). Tag release and recovery data from the RTTP-IO program were included in the model to inform abundance and fishing mortality rates. Several sensitivity models are presented to explore the impact of key data sets and model assumptions.

A model ensemble was proposed for quantifying the status of the stock which corresponds to a combination of model configurations, including alternative CPUE indices (PL, PSLs, and/or behaviour indices), alternative assumption on CPUE catchability (annual increase of 0 or 1%), alternative values of SRR steepness (0.7, 0.8, or 0.9), alternative growth parameter options (L^∞ fixed or estimated). The model ensemble (a total of 36 models) encompassed a range of stock trajectories and was aiming to address some of the major uncertainty in key data datasets and productivity parameters. Estimates of stock status were combined across the 36 models and incorporated uncertainty estimates from individual models as well as across the model ensemble.

There has been a substantial increase of fishery dependent abundance index in recent years: the CPUE from the Maldivian Pole and line fishery increased by 75% from 2019 to 2022, and the PSLs also increased by over 30% between 2019 and 2021. As the overall catches for skipjack have been remaining high, the increase in abundance was driven primarily by an increase in recruitment which was estimated to be much above the long-term average. As such the overall stock status estimate is substantially more optimistic than the previous assessment, with the median estimate of current depletion increasing from 45% (SB₂₀₁₉/SB₀) in the 2020 assessment to 53% B₀ (SB₂₀₁₉/SB₀) in the current assessment. Spawning stock biomass in 2022 was estimated to be 230% of the level that can support MSY ($SSB_{2022}/SSB_{MSY} = 2.30$). With high likelihood, current fishing mortality was estimated to be lower than F_{MSY} ($F_{2022}/F_{MSY} = 0.49$). The probability of the stock being currently in the green Kobe quadrant is estimated to over 95%. Considering the quantified uncertainty, the stock is considered not to be overfished and is not subject to overfishing in 2022. The retrospective analysis provided some confidence on the robustness of the model with respect to recent data. However, the catches in the last two years have exceeded the catch limit set for 2021 – 2023 and are also higher than the estimated MSY. The estimated stock status is summarized as below:

• Catch in 2022	648 695
• Average catch 2017–2022	601 499
• MSY (80% CI)	584 774 (512 228–686 071)
• F_{MSY}	0.99 (0.71–1.42)
• $F_{40\%SSB}$	0.55 (0.48–0.65)
• SB ₂₀₂₂ :	1 142 919 (842 723–1 461 772)
• SB _{MSY}	513 831 (369187–678936)
• SB ₂₀₂₂ /SB ₀	0.53 (0.42–0.68)
• SB ₂₀₂₂ / SSB _{MSY}	2.30 (1.57–3.40)
• F_{2022} / F_{MSY}	0.49 (0.32–0.75)

1. INTRODUCTION

The Indian Ocean skipjack tuna (*Katsuwona pelamis*, SKJ) fishery is one of the largest tuna fisheries in the world, with total catches of 400-600 thousand tons over the past decade. Some bioeconomic modelling of the fish population and fishery was undertaken a few years ago (Mohamed 2007). Before 2010, management advice has relied on data-based indicators, and mortality estimates from analyses of the recent RTTP-IO tagging data (Edwards et al. 2010). A full integrated model-based assessment was developed in 2011 (Kolody et al 2011), and further updated in 2012, 2014 (Sharma et al. 2012, 2014), 2017, and 2020 (Fu 2017, 2020). In 2016, the IOTC commission adopted a Harvest control rule (HCR) for the skipjack tuna through Resolution 16/02 (IOTC 2016). The HCR recommends a total annual catch limit inferred from a relationship between stock status (spawning biomass relative to unfished levels) and fishing intensity (exploitation rate relative to target exploitation rate) estimated from a model-based stock assessment.

Previous skipjack tuna assessments have investigated the impact of a range of data and model assumptions (e.g., spatial and temporal structure) on estimates of stock status and a systematic approach was taken to evaluate interactions of model assumptions and to develop management advice. In 2017, the WPTT19 agreed to a final ensemble of 37 models to characterize key uncertainties related to steepness, natural mortality, tagging program, tag mixing period and tagging mortality (IOTC 2017); In 2020, WPTT22 adopted a full factorial uncertainty grid that include alternative spatial structure, steepness, tag data weights, and CPUE catchability assumption. The median estimate from each set of stock assessment model ensemble was then used to determine the catch limits to be implemented over the next three years through the HCR (470,029 tonnes of 2021-2020 and 513,572 tonnes for 2021-2023).

The HCR described in Resolution 16/02 requests that the skipjack tuna stock assessment is conducted every three (3) years, with the next stock assessment scheduled in 2023. In this context, this report provides an update and further development of the integrated stock assessment for skipjack in the Indian Ocean. The model incorporates three additional years of data (2020–2022), improved information on nominal catches from IOTC database, and revised CPUE time series for the Maldives Pole and line and European Purse seine fleets. The assessment provides estimates of population parameters, stock status and reference quantities (required for the calculation of the catch limit from the HCR), with uncertainties characterised through a model grid on combinations of model settings and parameter values. The assessment builds on the work by Fu (2017, 2020), Sharma et al. (2012, 2014), and Kolody (2011), and uses a size based, age structured population model, implemented in Stock Synthesis 3 (Methot and Wetzel 2013, Methot et al. 2020).

1.1 Biology and stock structure

Skipjack are the smallest of the major commercial tuna species and are found mainly in the tropical areas with geographic limits between 55-60° N and 45-50° S. Skipjack are highly fecund and can spawn year-round over a wide area of the tropical and subtropical waters. Environmental conditions (such as sea surface chlorophyll) are believed to significantly influence recruitment and can produce widely varying recruitment levels between years (Marsac 2023). The historical Japanese surveys of skipjack larvae have identified large quantities of skipjack larvae in the Equatorial Eastern IO (Nishikawa et al 1985), but these surveys have been quite rare in the Western IO. The location of skipjack nurseries remains widely unknown, as well as the biology of skipjack early juveniles, because very small sizes of skipjack have never been exploited significantly in the IO (Fonteneau 2014).

A substantial amount of information on skipjack movement is available from tagging programs, which have documented some large-scale movement within the Indian Ocean. The average range of movement during the skipjack lifetime can be estimated at about 1000 miles, with maximum distance of about 2000 miles (Fonteneau 2014). Skipjack movement is highly variable and is thought to be influenced by large-scale oceanographic variability (Mackenzie et al. 2016).

Genetic analyses by Dammannagado *et al.* (2011) have suggested that there might be two (or more) skipjack populations in the Indian Ocean. A recent stock structure study based on analysis of the shape

of otolith from four areas south of Java showed that they are not statistically different among regions, suggesting that these skipjack belong to a single stock (Wujdi et al. 2017). However, Due to the limited spatial range of the samples, this conclusion cannot be applied to the whole Indian Ocean. Using next generation genetic sequencing, Grewe (2019) suggested a weak genetic population differentiation of skipjack tuna from the central Indian Ocean through to the Eastern Pacific Ocean.

1.2 Fishery overview

The Indian Ocean skipjack catch history is shown in Figure 1. Catches increased steadily from the 1980s to a peak at over 600,000t in 2006, but have been decreasing since the mid-2000s. Since 2006 total catches have declined to around 340,000t in 2012 although since 2013 catches have increased sharply and in 2018 reached again a level of 600,000t mostly driven by the purse seine (associated school) fisheries. The catches dropped in 2019 and again in 2020 to about 550 000 t but increased to a historical peak at 655,000 t in 2021. The annual catches 2018 – 2022 have all exceeded the catch limit as set out by the skipjack Harvest Control Rule. Figure 2 illustrates the spatial distribution of the catches from the main fisheries (purse seine, pole and line, gillnet, line). In 2022, purse seine accounted for about 53% of the total catches, with the remainder of catches mainly taken by the pole and line (20%), gillnet (18%) and line (7%) fisheries (IOTC 2023).

The Maldives has sustained a pole and line (PL, bait boat) skipjack fishery for many centuries, with catches increasing dramatically with the uptake of mechanization and deployment of larger vessels (more poles, larger bait and storage capacity, longer range) starting in the 1980s. The Maldives has experienced substantial catch declines since the peak in 2006, for reasons that are not entirely clear. Adam (2010) suggests that this may reflect declining skipjack abundance, limitations to bait availability or changing economic incentives (e.g., high fuel prices). There has been an increasing trend in catch levels from 2018, with a slight drop in 2019 followed by a new increase in catches which peaked at 128,000 t in 2021 (IOTC 2023).

There has been a rapid increase in skipjack catches with the introduction of the purse seine fleets in the 1980s, and the development of the fishery in association with Fish Aggregating Devices (FADs) since the 1980s (e.g., Chassot 2010, Delgado de Molina 2010). The European/Seychelles PS catch has fluctuated considerably since around 2000 without a clear trend. Catch declines in the recent years are probably partly attributable to the effects of piracy in the prime fishing area near Somalia. From 2003-06 the decline was due to very good fishing of large yellowfin tuna on free schools. After 2007 piracy or other ‘unknown’ reasons may be the cause of the decline. In recent years, well over 90% of the skipjack tuna caught by purse seine vessels are taken from around FADs. The fraction of catches from FAD associated schools was around 98% of skipjack catches reported in 2018 and around 96% in 2021.

Several fisheries using gillnets have reported large catches of skipjack tuna in the Indian Ocean, including the gillnet/longline fishery of Sri Lanka, driftnet fisheries of I.R. Iran and Pakistan, and gillnet fisheries of Indonesia. In recent years gillnet catches have represented as much as 20% to 30% of the total catches of skipjack tuna in the Indian Ocean. Moderate catches are taken by the line fishery representing a mixture of gears using handlines, trolling, and small longlines, mostly in the eastern Indian Ocean (Figure 2).

A substantial portion of the total catch is taken by a mix of artisanal gears, with minor catches dating back before the pre-industrial period. For the assessment, these fleets have been pooled together, in the heterogeneous *Other* fleet. The bulk of the recent catch in this fishery is from the small purse seiners fisheries of India, Indonesia, Malaysia, and Mozambique. These fleets were mostly operating in coastal waters. The aggregate catches of these fleets have been increasing more recently.

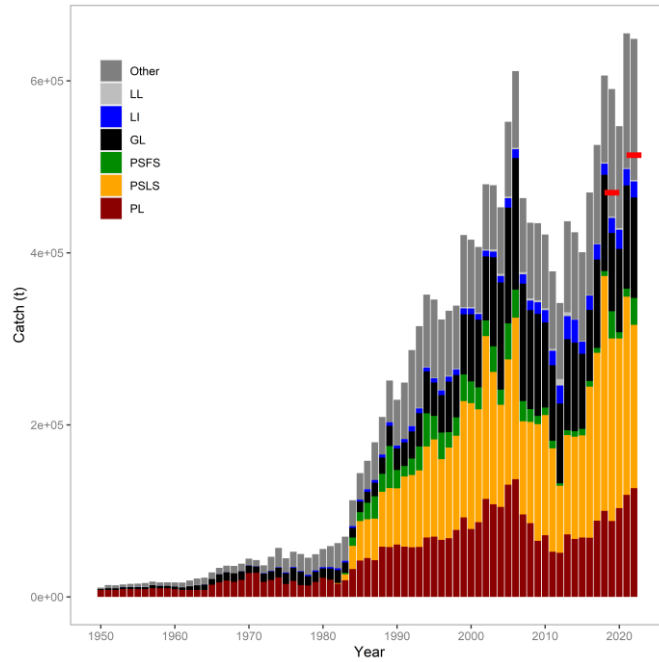


Figure 1: Total annual catch (1000s t) of skipjack tuna by fishery from 1950 to 2022. The red line indicates the catch limit of 470,029 t and 513,572 t established by the HCR for 2018–2020 and 2021–2023 respectively. Gear codes are described in Section 2.3.

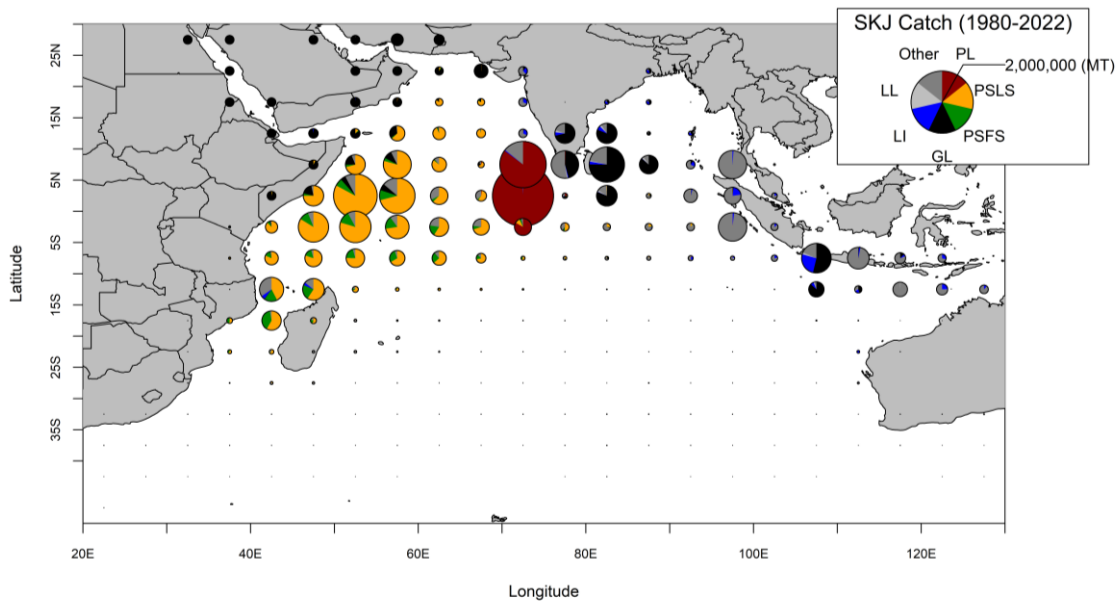


Figure 2: Spatial distribution of Indian Ocean skipjack catches by main fisheries aggregated for 1980-2022. Gear codes are described in Section 2.3.

2. OBSERVATIONS AND MODEL INPUTS

Data used in the stock assessment of skipjack tuna consist of catch, length frequency data for the fisheries defined in the analysis, relative abundance indices and tag-recapture data. The details of the configuration of the fishery specific data sets are described below.

2.1 Spatial stratification

The assessment assumed that the entire Indian Ocean as one homogeneous area, with the different fisheries harvesting different portions of the skipjack population. The tagging data suggest that SKJ migrate quickly but the limited distribution of tag releases, and small number of returns outside of the European/Seychelles purse seine fleets (mainly operating in the western equatorial Indian Ocean) makes it difficult to quantify large-scale movements. It is notable that basin-scale movements into the eastern Indian Ocean were observed from the EU/Seychelles fleet, but proper mixing might never occur at the basin scale. Thus, the inclusion of the tagging data in the aggregated spatial structure may induce bias due to the low mixing rates. Another concern is that Maldives PL CPUE is used as an index of abundance for the broader population in the aggregated model when in fact it is derived from the relatively small area of the Maldives EEZ.

The previous assessment included a two-region spatial structure which assumed discrete populations west and east of 80° (see Figure 2 of Fu 2020). The partition is based on the distribution of major fisheries and appears well fitted with geographical scale of the observed skipjack movements in the western Indian Ocean. The partition allows for spatial heterogeneity in tag mixing and changes in abundance (the mixing rate is probably quite low between the Northern and southern western Indian Ocean, see Fonteneau 2014). However, there is a lack of information on regional scaling (Hoyle and Langley 2018) to estimate the biomass distribution across the two regions because the purse seine and pole and line indices, which are assumed to index regional abundance, are not comparable in relative size. The tagging data contains little information about migration between the east and western Indian Ocean. These factors led to significant variations and uncertainty in estimates of regional abundance and movement rates across an array of model options. The spatial model requires further development and is not used in the current assessment.

2.2 Temporal stratification

The population was assumed to be in unfished equilibrium in 1950, the start of the catch data series. The model was iterated from 1950 to 2022. The population dynamics were represented with an annual/season configuration, referred as the SS3 internal year-season (SSYS). The model was iterated on an annual time step which is split into four quarters to represent potentially important seasonal processes. The tag ages are assigned to annual increments and recruitment is apportioned among four seasons from a single recruitment event. The previous assessments also examined an alternative configuration (Calendar Season as Model Year, CSMY) which is commonly used for species with rapid dynamics such as tropical tuna. The CSMY defined quarterly time periods as years, i.e., each model “year” is a three-month period, and each age class is 3 months (see Fu 2017 for a detailed comparison of the two temporal structure). For this assessment, only the SSYS structure is used for all models.

2.3 Definition of fisheries

SS3 requires the definition of fisheries that consist of fishing units with similar selectivity and catchability characteristics. Seven fleets were defined on the basis of gear and fleet of operation:

1. PL – Maldivian Pole and Line fleet.
2. PSLS - FAD/log associated Purse Seine (PS) sets from the EU/Seychelles fleets.
3. PSFS - unassociated PS sets from the EU/Seychelles fleets.
4. Gillnet - includes primarily gillnet fleets from Sri Lanka, Iran, Indonesia and Pakistan
5. Line - includes primarily handline and small coastal longline gears from Yemen, Sri Lanka, Maldivian, and Madagascar.
6. Longline – a trivial catches from Distant water longline fishing fleets
7. Other – includes all other fleets, primarily non-EU/Seychelles PS fleets, trolling, and small coastal fleets (e.g. ring nets).

In the earlier assessments, the “Other” fleet was defined broadly to have aggregated gillnet, line, longline fisheries (in total four fisheries were defined for the assessment). Consequently, the ‘Other’ fishery included a heterogeneous mix of fleets which caught different sizes of fish (e.g., the longline

generally caught much larger skipjack than other gears). The combined size distribution was unlikely to be representative of this composite fleet if the component fisheries had inconsistent size sampling over time. Therefore, it was decided to partition this composite fleet into fisheries with distinctive selectivity characteristics, with the aim to improve predicted sizes in the catch and the estimates of the selectivity patterns (Fu 2020).

2.4 Catch history

The total catches were calculated by the Secretariat (IOTC 2023). The nominal catches are not always reported by species and/or gear by the responsible institutions in each country. The catches reported under species and/or gear aggregates are decomposed by the IOTC secretariat using alternative sources of information (if available), or a pre-defined criterion so that all catches are separated into individual gears and species. The catch time series for the 7 fleets is shown in Figure 1. Total Skipjack catches in the years 1987-2018 have been relatively impacted by the revisions introduced to the official catch series submitted in late 2019 by Pakistan for its gillnet fisheries, with revised catches being now 69,244 MT lower (in total) during considered years (IOTC 2020).

2.5 CPUE indices

2.5.1 Maldives PL CPUE series

Medley et al. (2023) updated the abundance index for skipjack tuna from Maldives pole and line catch and effort data. The index was derived from multiple datasets with differing level of detail over the period 1995–2023 using a Bayesian approach (Figure 3). The main concern on this CPUE is that the spatial area in which the Maldives pole and line operates may not represent the Indian Ocean, and thus the index may be more appropriate as a regional abundance index. There has been a significant and sharp increase of the index since the last assessment, with the index in 2022 being 75% higher than in 2019.

2.5.2 EUROPEAN PSLS abundance indices series

The European and associated flags purse seine fishing activities in the Indian Ocean during 1981–2020 have been monitored through the collection of logbook and observer sampling. Standardized indices of the abundance of skipjack caught by the European purse seiners (Spain and France) under floating objects (including primarily sets on drifting fishing aggregating devices) was developed (Kaplan, et al. 2023). The standardization was based on the application of a generalized additive mixed model (GAMM) which considered a comprehensive list of candidate covariates, including non-conventional covariates. Both a short time series from 2010 to 2021 and a long time series from 1990 to 2021 were developed (the short time series includes several methodology improvements that make use of newly available information). The short series closely resembles the long series across comparable periods, but it is insufficient to be used as an independent index in the model (using the short series would yield results that are very similar to those of the long series in the model that included both the PL and PSLS index). Consequently, the assessment focuses on the long timeseries. The index has seen a significant increase in the last two quarters of 2021, which is about 50% higher than average of 2019-2020.

2.5.3 Other abundance indices

Baidai et al. (2023) developed a novel approach to construct estimates of tropical tuna population size based on their associative dynamics with floating objects and acoustic data collected from echosounder buoys. The approach was implemented to provide time series of abundance for skipjack tuna in the western Indian Ocean, over the period 2013 to 2021 (Figure 3).

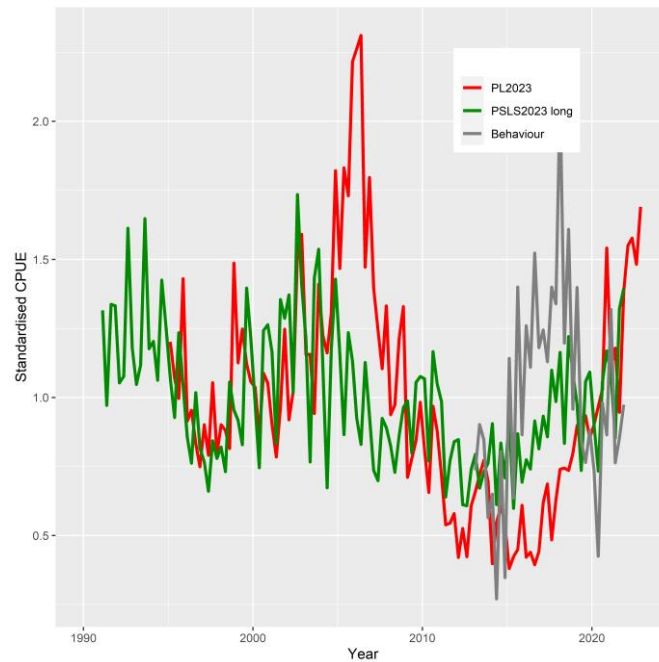


Figure 3: Relative abundance indices for skipjack tuna: standardised CPUE indices from the Maldives PL fisheries 1995 – 2022 (PL); standardised CPUE indices from the European PS associated schools 1991 – 2021 (PSLS); indices based on associative dynamics with floating objects and acoustic data 2013 – 2021 (Behaviour).

2.6 Length frequency data

Available length-frequency data for each of the defined fisheries were compiled into 27 3-cm size classes (20–22 cm to 98–100 cm) and were aggregated to provide a composite length composition for each year/quarter. Each length frequency observation for purse seine fisheries represents the number of fish sampled raised to the sampling units (sets in the fish compartment) while for fisheries other than purse seine each observation consisted of the actual number of skipjack tuna measured. In the assessment, all length composition strata from all fleets were weighted by dividing the number of fish included in the aggregated sample by a factor of 1000, with a maximum initial sample size of 10, The *Other* fleet was down-weighted to have a maximum initial sample size of 1, because it represents a heterogeneous mix of fisheries, many of which are poorly sampled. Size data has been examined by the Secretariat and problematic data were removed from the database (country-gear-time-area strata for which the size data are removed can be made available upon request). For example, Maldivian PL from 1987 to 2000 have been removed from the database as they are considered extremely unreliable. Similarly, the data for 2015/2016 was removed as only extremely small fish (less than 1kg on average) were reported. Aggregated catch-at-length distributions for each fishery are shown in Figure 4.

The Maldives PL fishery length distribution typically has two very distinct modes (about 50 cm and 70 cm) indicating that the fishery appears to be catching two different life stages of skipjack tuna. The multimodal length frequency can introduce a significant amount of uncertainty into the assessment model because that changes in the composition of modes imply changes in selectivity. Before 2015, the two modes are highly distinct, but then became less obvious after 2016 (Figure 4). Further investigation was done on the spatial and temporal distribution of the Maldives PL length samples (provided by 1x1° resolution). Prior to 2015, all samples were collected from a few spots along longitudes 72° to 73°. The multimodal distribution is mainly driven by samples from one spatial grid cell (0.5° latitude and 73.5° longitude 73.5), which accounted for over 30% of total samples. After 2016, the samples were taken from a considerably wider range of locations and contains mainly smaller fish. The multimodal distribution doesn't appear to be seasonal.

The recent decline in mean size in the *Other* fleet probably reflects the erratic sampling from this fleet. It has been noted previously that the length frequency data from Thailand small purse seiners in 2007

and following years were of extremely poor quality. For the ‘Other’ category, size data between 2007 and 2010 were not used.

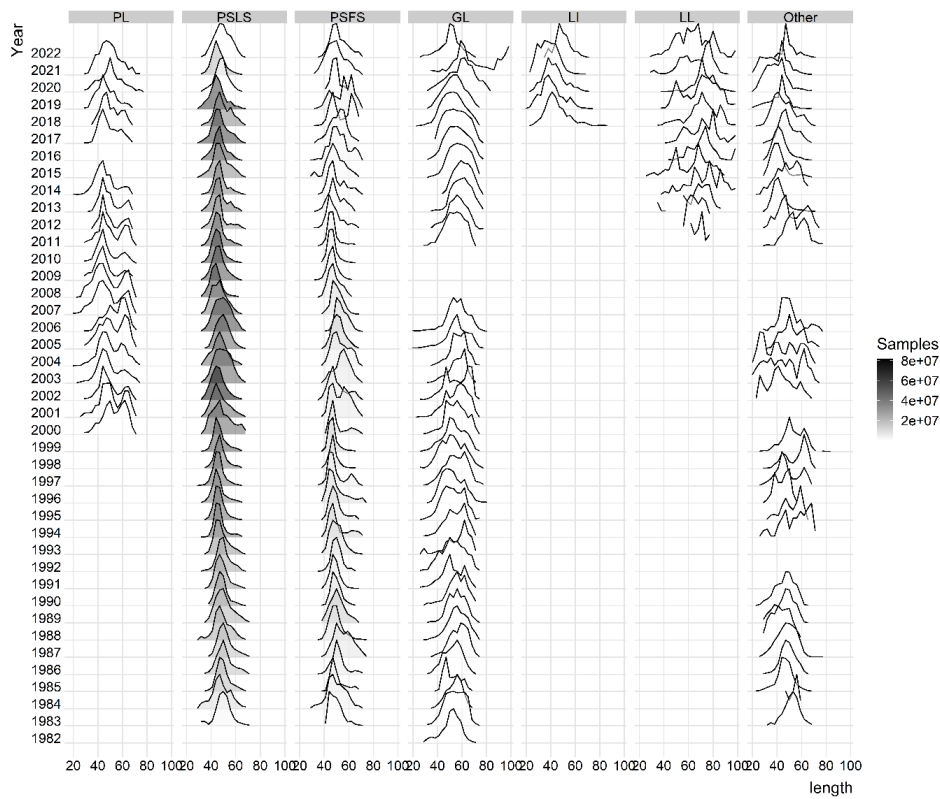


Figure 4: Length compositions of skipjack tuna samples aggregated by year and fishery.

2.7 Tagging data

A considerable amount of tagging data was available for inclusion in the assessment model (Hallier & Million 2009). Between 2005 and 2007, about 77000 tagged skipjack were released from Tanzania, Seychelles and Mozambique Channel under the RTTP-IO program (Figure 5). Additional tagging (~22000 releases) also occurred in the eastern Indian Ocean as part of small-scale tagging operations in 2004–2009 (Figure 5). The most substantial small-scale project was based in the Maldives (Jauharee & Adam 2009), but tags were also released near Lakshadweep, Mayotte, western Sumatra and the Andaman Islands.

Most skipjack tagged under the RTTP-IO were under 2-year of age (Figure 6) The percent of returns for the RTTP-IO tags is approximately 16% and the returns were primarily from the purse seine fishery in the western Indian Ocean within four years after release (Figure 7, Table 1). A significant proportion of the tag returns from purse seiners were not accompanied by information concerning the set type. These tag recoveries were assigned to either the free-school or FAD fishery based on the proportion of catch by each fishing mode. The low number of returns from other fisheries is partly due to lower catch numbers, particularly of the smaller size classes that were tagged, but probably due in most part to non-reporting (Eveson 2012 et al.).

In contrast smaller fish was tagged under the small-scale program (Figure 6) and the percent of tag returns is approximately 12% (Table 1). The returns were primarily from the Maldives Pole and line fishery (Figure 7), but the numbers were variable over time. In general release cohorts with higher recovery rates were mostly tagged in Maldives waters 2007 – 2009, whereas releases made further east in the IO waters between 2004 and 2006 tend to have lower recovery rates. The recovery from the purse seine fishery is extremely low (less than 10 recoveries except for those released in the first two quarters of 2009).

The RTTP-IO data is considered more reliable than the small-scale tagging programs, because the RTTP-IO has a much larger number of tags and was released by more experienced taggers. In contrast, there was no tag shedding estimates for the fleets conducting the small-scale tagging programs, and the reporting rates from pole and line fishery were also unknown. The previous assessment included the small-scale data in part of the model grid considering that the small-scale tagging program may provide additional insight into spatial dynamics. However, the inclusion of the small-scale data is likely to introduce bias to the model estimates because (1) the recovery rate of small scale tags from the PS fishery is extremely low (the tag returns from the PS fishery is the primary source of information on abundance), and (2) very few tags (<5%) were recovered with a time of liberty exceeding 2 quarters, whereas it is generally agreed that longer periods are required to achieve sufficient tag mixing. The utility of small-scale tag data was thoroughly investigated in previous assessments and they are not included in the current assessment.

For incorporation into the assessment model, tag releases were stratified by release region, time period of release (quarter) and age class. The returns from each tag release group were classified by recapture fishery and recapture time period (quarter). The tag data were further adjusted for tag losses and reporting rates to minimize the bias on estimates of fishing mortality and abundance in the assessment model. The procedure is described in below.

Age assignment of tag release. The length of release of each tag is recorded in the database but the model dynamics are based on ages. The age of each individual tag was estimated from the mean of the growth curve, assuming a 1 January birthdate. The age estimation occurs external to the model.

Tagging mortality. The number of tags in each release group was reduced by 25% to account for initial tag mortality. Tagging mortality was estimated relative to those for the best tagger (Hoyle *et al* 2015). Hoyle *et al.* (2015) did not find any differences in tagging induced mortality between species in the Indian Ocean but tag mortality was estimated to be lower for skipjack in the Pacific Ocean where there are more data.

Reporting rate. The results of the tag seeding experiments conducted during 2005–2008, have revealed considerable temporal variability in tag reporting rates from the IO purse-seine fishery (Hillary *et al.* 2008a). Reporting rates were lower in 2005 (57%) compared to 2006 and 2007 (89% and 94%). Quarterly estimates were also available and were similar in magnitude (Hillary *et al.* 2008b). This large increase over time was the result of the development of publicity campaign and tag recovery scheme raising the awareness of the stakeholders, *i.e.* stevedores and crew. SS3 assumes a constant fishery-specific reporting rate. To account for the temporal change in reporting rate, the number of tag returns from the purse-seine fishery in each stratum (tag group, year/quarter, and length class) were corrected using the respective estimates of the reporting rates. Following Kolody (2011) and Fu (2017), tags recovered at-sea are assumed to have a 100% reporting rate; tags recovered from landings in Seychelles were corrected for the quarterly estimates of reporting rates from Hillary *et al.* (2008b). The tag recoveries were further increased by the proportions of EU PS catches landed outside the Seychelles, to account for purse-seine catches that were not examined for tags. For example, the adjusted number of observed recaptures for a PSLS fishery as input to the model, R'_L was calculated using the following equation:

$$R'_L = R_L^{sea} + \frac{R_L^{sez}}{p^{sez}\gamma^{sez}}$$

where

R_L^{sea} = the number of observed recaptures recovered at sea for the PSLS fishery.

R_L^{sez} = the number of observed recaptures recovered in Seychelles for the PSLS fishery.

r^{sez} = the reporting rates for PS tags removed from the Seychelles

P^{sez} = the scaling factor to account for the EU PS recaptures not landed in the Seychelles.

The adjusted number of observed recaptures for a PSFS fishery was calculated similarly. A reporting rate of 94% was assumed for the correction of the 2009–2015 tag recoveries. The numbers of tag recoveries were also adjusted for long-term tag loss (tag shedding) based on an analysis by Gaertner and Hallier (2015). Tag shedding rates for skipjack tuna were estimated to be approximately 3% per annum.

For the RTTP-IO, a total of 58 420 releases were classified into 40 tag release groups. Most of the tag releases were under age 2 (Figure 6) A total of 10458 actual tag recoveries were included in the tagging data set. The cumulative effect of processing the tag recovery data increased the number of recoveries to 11,640 tags.

Table 1: Number of Tag releases by year (of release) and recoveries by year (of recovery) for the skipjack tuna RTTO-IO and small scale tag Programs.

RTTP Release		Recovery							
		2004	2005	2006	2007	2008	2009	2010	2011
2005	14744		160	1592	277	26	2		
2006	41387			2793	4277	303	39	5	
2007	21741				1901	1019	167	9	
SS Release		2004	2005	2006	2007	2008	2009	2010	2011
2004	4339	254	39	6	3	2			
2005	2208		51	35	3				1
2006	2883			176	19	2			3
2007	741				29	19	8	3	
2008	5029					383	180	2	
2009	7233						1440	39	2

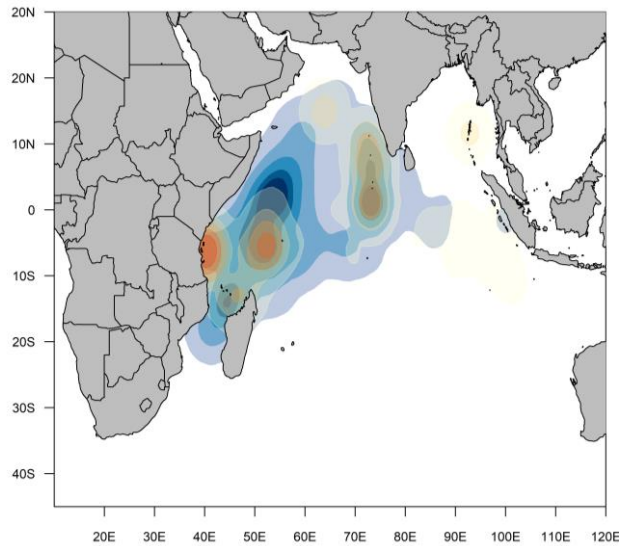


Figure 5: Location of releases (red) and density of recoveries for the skipjack tuna RTTO-IO and small-scale tag Programs

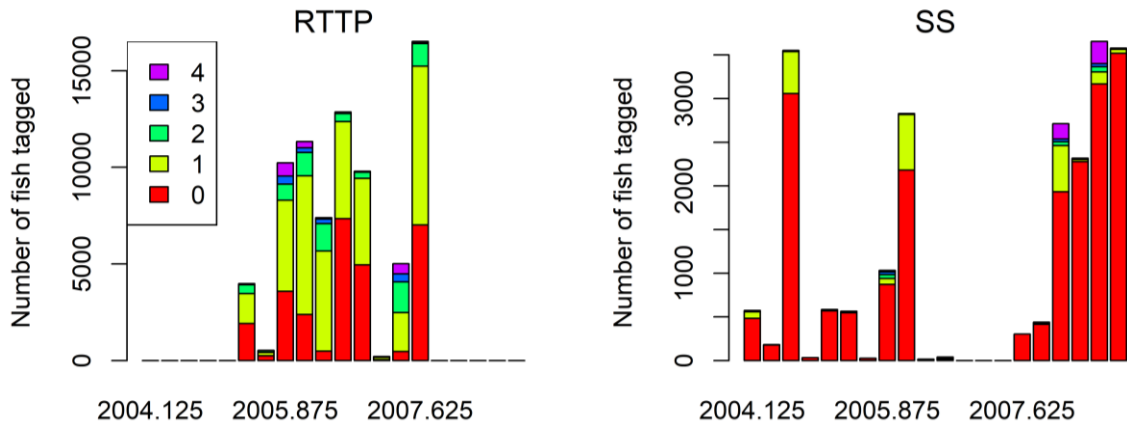


Figure 6 : Number of tag releases quarter and age class for the skipjack tuna from the RTTO-IO and small-scale tag Programs. Ages were assigned based on the length.

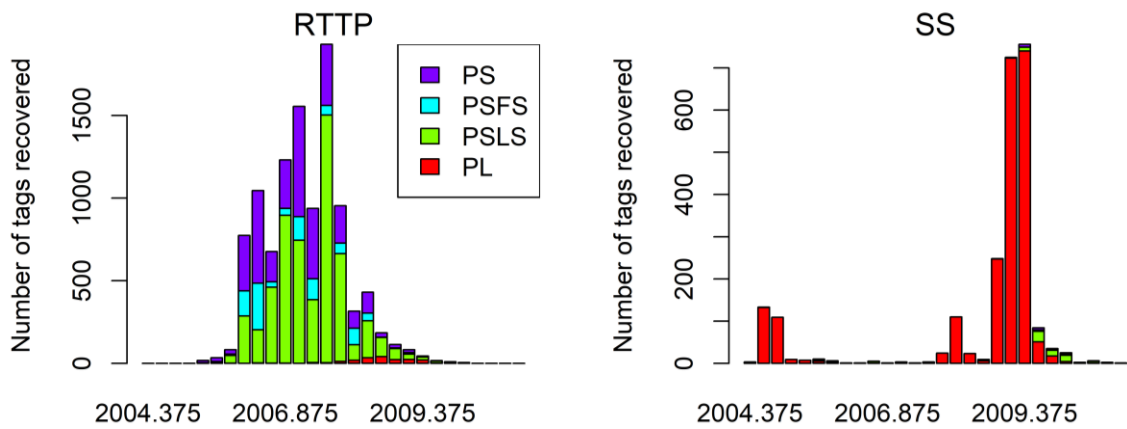


Figure 7: Number of tag recoveries by year/quarter and fishery for the skipjack tuna from the RTTO-IO and small-scale tag Programs. Purse seine tag recoveries have not been corrected for reporting rate.

3. MODEL STRUCTURAL AND ASSUMPTIONS

3.1 Population dynamics

The model was sex-aggregated (and reported spawning biomass is the summed mass of all mature fish). The stock assessment model partitioned the Indian Ocean skipjack age groups 0–8 years with the last age a plus group (in unfished equilibrium, <0.25% of the population survives to reach the plus-group with the constant M value considered).

The population was assumed to be in unfished equilibrium in 1950, the start of the catch data series. The model was iterated from 1950-2022 using a quarterly time-step. The nominal unit of time in the model is one year during which population processes (e.g., recruitment, spawning, and ageing) were applied in sequence according to the dynamics implemented within the Stock Synthesis model (Methot 2013). The Observations were fitted to model predictions on the seasonal basis within the year.

An alternative model option commenced in 1970 and assumed an exploited, equilibrium initial state, considering that the main fisheries were developed after 1970 and there is almost no data prior to that. Initial fishing mortality parameters were estimated for each of these fisheries, based on early catches. The resulting fishing mortality rates are applied to determine the initial numbers-at-age. This model option yielded very similar results and thus was not reported further.

3.1.1 Recruitment

For some of the tuna species there is an indication of a strong seasonal pattern in recruitment. However, Itano (2000) suggested tropical tuna spawning does not always follow a clear seasonal pattern but occurs sporadically when food supplies are plentiful. SKJ has been assumed to have a continuous spawning season.

Recruitment was assumed to occur annually at the start of the year and the SS3 will allocate recruitment to each season (the population will have a collection of seasonal cohorts with different birthdays), with the proportion being estimated as time-varying parameters. New recruits enter the population as age-class 0 fish (averaging approximately 20 cm). A Beverton-Holt stock recruitment relationship was assumed with steepness fixed at a range of options. ISSF (2011) summarises steepness estimates from tuna fisheries, the high values reported seem to be consistent with SKJ life history. The final model options included three (fixed) values of steepness of the BH SRR (h 0.7, 0.8 and 0.9). These values are considered to encompass the plausible range of steepness values for tuna species and are routinely adopted in tuna assessments conducted by other tuna RFMOs.

Annual deviations from the stock-recruitment relationship were estimated for 1983–2021, assuming a lognormal distribution. Assessments of major tropical tuna species using a quarterly model time-step typically assumed the quarterly recruitment events to have a fixed standard deviation (σ_R) of 0.6 for recruitment deviates (Kolody et al. 2018), corresponding to an annual CV of about 0.3 (assuming quarterly recruits are independent, and the annual recruitment is calculated as the mean of four seasonal events). Season-specific parameters were estimated to distribute the mean recruitment among seasons (quarter). Recruitment anomalies by season were estimated for 1983 – 2021 with a standard deviation of 0.3.

3.1.2 Growth and Maturation

Skipjack growth is rapid compared to yellowfin and bigeye tuna. Young skipjack is approximately between 10–20cm as age of 40–90 days after hatching and immature fish is approximately in a range of 20 cm to 40 cm as age of 90 days to one year after hatching (Kiyofuji et al. 2019). Earlier assessments have considered length-at-age relationships that followed the standard von Bertalanffy growth function. But there were concerns that the von-B growth curves might not be capturing the rapid initial growth rate for this species (e.g. Kayama et al. 2004). The 2017 assessment adopted a two stanza VB-logK curve of Eveson (2012), derived from the tag-recapture data. The VB-logK curve was approximated using a Richards curve in SS3, with $L^\infty = 70\text{cm}$, $k=0.34$, and the inflexion parameter fixed at 2.96.

However, the L^∞ appears to be low compared to the Pacific, where a number of estimates suggested maximum length above 80 cm. The two-stanza growth is considered to be appropriate for skipjack tuna as it captures the rapid growth of juveniles, and diminished growth from a transfer of energy from somatic growth to gonad development (Grande et al. 2010). A CV of 0.2 and 0.1 is assumed for the length at the initial and maximum age, respectively with linear interpolations for intermediate ages (Figure 8–left), loosely based on evidence from tagging data.

Maturity was estimated by Grande *et al.* (2010): invariant over time with 50% maturity at length 38 cm (Figure 8–right), corresponding to an age-at-maturity of 0.4 y with the Richard growth curve. This is also very similar to the 40 cm value reported in the Pacific, where the maturity is estimated to follow a knife-edge pattern with all fish two quarters or less being immature and all fish older being fully mature (Vincent et al. 2019). The weight-length relationship was estimated from Chassot et al. (2016), where $W = 4.97e-006 L^{.39292}$.

Grande et al. (2010; 2014) studies used the ‘cortical alveolar’ oocyte development stage and above as the threshold indicating a fish was mature. A slightly updated ogive was estimated by Grande et al. (2014) with L50 at 39.9 cm FL. Zudaire et. al (2022) estimated reproductive parameters for skipjack tuna in the Indian Ocean as part of the ‘GERUNDIO’ project. The estimate of L50 (41.3 cm FL) obtained in this study is slightly higher than that obtained by Grande et al. (2010; 2014). probably affected by different maturity thresholds used in both studies.

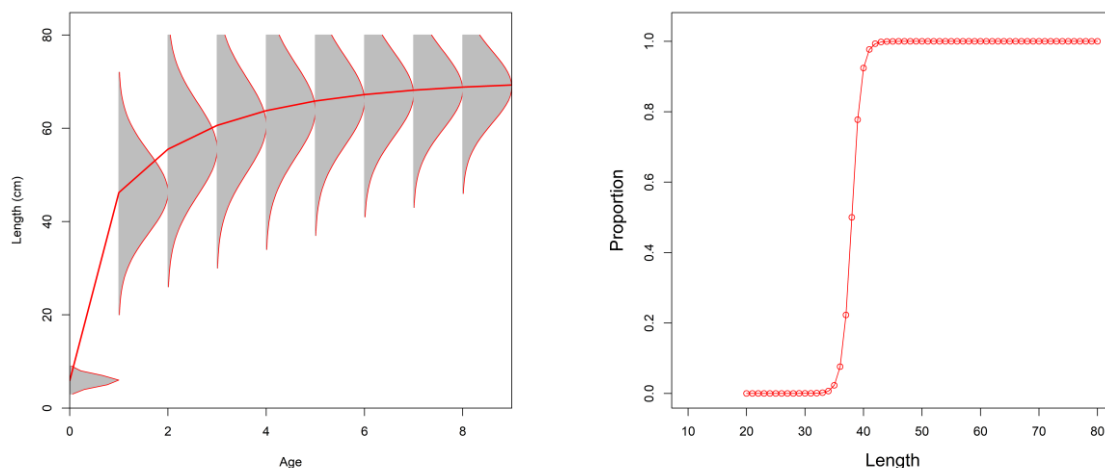


Figure 8: Fixed growth function for skipjack tuna following Eveson et al. 2012 (left) and length-based maturity Ogive following Grande *et al.* (2010). For the growth function, the red line represents the estimated mean length (FL, cm) at age and the grey area represents the assumed distribution of length at age).

3.1.3 Natural mortality

Independent estimates of natural mortality for skipjack tuna were available from tagging data (Everson 2011) but the estimates appeared to be very low compared to the assumed or estimated M in the other oceans. For the assessment, the natural mortality of 0.8 (constant across all ages) is used, which is equal to the value used by the ICCAT). Previous assessment also considered estimating M within the model when the small-scale tagging data were included, and the estimates were similar in magnitude to the assumed value of 0.8.

3.2 Fishery dynamics

Length based selectivity were assumed for all fisheries. Within the model, the length-based selectivity is used to calculate the predicted catch-at-length distribution. Selectivity is internally converted to an age-based selectivity for purposes of removing the appropriate portion of the population in the catch. A

non-parametric, cubic spline function was estimated independently for the selectivity of pole and line, and purse seine fleets (both PSLS and PSFS). The function is flexible enough to represent polymodal functions (and was motivated by the clear bimodal distribution of the PL fleet). Seven nodes were estimated for the PL fleet, and 5 nodes for the PSLS, PSFS fleets. The selectivities of the Gillnet and Line fisheries were estimated using a dome-shaped, double normal functional form, and the selectivity of the longline fisheries was estimated using a monotonically increasing, logistic function.

Fishing mortality was modelled using the hybrid method that estimates the harvest rate using Pope's approximation and then converts it to an approximation of the corresponding F (Methot & Wetzel 2013).

3.3 Dynamics of tagged fish

In the population model, tagged fish are assumed to have identical dynamics to the general population. Therefore, a reasonable period of mixing is required before this assumption would be valid. Tag displacement appears to suggest rapid mixing within the core PS area. However, this would be contingent upon the distribution of fishing effort (i.e., if the gear is deployed a long way from the release site, all recoveries will suggest rapid movement, but they might not represent the movement of the general population). Also, directed seasonal migration can cause large displacements, without necessarily resulting in uniform mixing. The Stock Synthesis model specifies a tag mixing period during which observations do not contribute to the overall likelihood function. Previous analyses examined tag mixing periods ranging from 2 to 6 quarters, with a longer mixing period effectively de-weighting the tagging dataset. The current assessment model used a four-quarter tag mixing period, retaining about 20% recovered tags in the model.

3.4 Modelling methods, parameters, and likelihood

The total likelihood is composed of four main components: catch data, the abundance indices (CPUE), length frequency data and tag release/recovery data. There are also contributions to the total likelihood from the recruitment deviates and priors on the individual model parameters. The model was configured to fit the catch almost exactly so the catch component of the likelihood is very small. There are two components of the tag likelihood: the multinomial likelihood for the distribution of tag recoveries by fleets over time and the negative binomial distribution of expected total recaptures across the model region.

Assumed CV of 20% (lognormal observation errors) was applied to standardised CPUE indices. The CV of 20% is probably not realistic for these fisheries, but it allows the model to fit the core features of the relative abundance series.

The individual length frequency observations was assigned a sample size that is proportional to the number of fish measured, with a maximum sample size capped at 10 (except for the 'Other' fisheries, where the maximum is capped at 1).

The negative binomial distribution allows for overdispersion relative to the ideal, independent movement, fully mixed, tag recovery distribution (e.g., which might be expected to conform to the Poisson distribution). The overdispersion parameter τ was fixed at 20 and was applied equally across all tag groups. Previous assessments attempted to estimate τ but the estimate was strongly driven by prior.

The parameters estimated by the model included:

- Catchability for the CPUE series
- Selectivity parameters
- Virgin recruitment
- Annual recruitment deviations from the stock recruitment relationship

- Annual seasonal-specific recruitment deviations

The Hessian matrix computed at the mode of the posterior distribution was used to obtain estimates of the covariance matrix, which was used in combination with the Delta method to compute approximate confidence intervals for parameters of interest.

3.5 Reference points

The harvest control rule for skipjack tuna as per IOTC Resolution 16/02 calculates a catch limit based on a relationship between stock status (spawning biomass relative to unfished levels) and fishing intensity (exploitation rate relative to target exploitation rate), to be estimated from a model-based stock assessment. The assessment therefore estimated the required inputs for the HCR, including SB2022/SB0 (current depletion), SB_{40%} (40% of unfished spawning biomass), F_{40%SSB} (fishing mortality corresponding to 40% of the unfished spawning biomass).

Provisions for interim reference points for skipjack tuna based on MSY are included in IOTC Resolution 15/10. Attempts to estimate MSY-related references in earlier assessments were not successful (Kolody et al. 2011) and as a result depletion-based proxies were used. The WPTT19 in 2017 uncovered an error in the definition of a selection curve that is thought to have caused a flat-top yield curve in some circumstances when F_{msy} cannot be calculated. Subsequent assessments have fixed the error. In the current assessment, MSY-based reference points are estimated and the stock status is reported in respect to the MSY-based target reference points in line with resolution 15/10.

4. ASSESSMENT MODEL RUNS

The approach is to explore a range of model assumptions and parameter configurations, and to examine areas of uncertainty that would impact assessment results. A basic model was identified for diagnostic purposes. Final model options included a grid of models running over permutations of plausible parameters and/or model settings, from which the uncertainty was quantified. The grid approach aims to provide an approximate understanding of variability in model estimates due to assumptions in model structure, which is usually much larger than the statistical uncertainty conditional on any individual model (McKechnie et al. 2016, Kolody et al. 2011). The assessment was conducted using the 3.30 version of the Stock Synthesis software. The stock status was reported for the terminal year of the model (i.e., 2022).

4.1 2020 model continuity run

In the 2020 assessment the final model options selected for management advice included 24 models with alternative assumptions on spatial structure, steepness, CPUE catchability, and tag data weighting. The model *io_h80_q0_tlambda01* (single region, steepness of 0.8, constant catchability, tag likelihood lambda of 1) was considered as a reference model (Fu 2020). The 2020 reference model was updated sequentially to ensure continuity, and to assess the influence of the revised and new data. The model period was extended to 2022 with incremental changes made to the observational data and other configurations (see Table 2 for details).

Table 2: Description of the sequence of model runs to update the 2020 reference model

<i>Model</i>	Description
<i>io_h80_q0_tlambda01</i>	2020 reference model
<i>1-update-catch</i>	Model extended to include 2020–2022, with updated catches
<i>2-update-LF</i>	Revised and updated length composition data for 2020–2022
<i>3-update-CPUE</i>	Revised and updated PL CPUE index 1995–2022, PSLs index 1990 – 2021
<i>Basic</i>	Extend period of estimation for recruitment deviates (to 2021); Definition of F-age for determination of MSY (2022);

--	--

4.2 Basic and sensitivity models

Minor revisions were made to the updated model to attain a basic model (Table 3), which served as a starting point for further exploratory, sensitivity analysis and the development of the final model ensemble. The basic and sensitivity models examined a range of model options related to the CPUE series, length composition and tagging data, biological parameters and model structure. The analysis complemented the suite of exploratory models conducted previously, with the goal of determining a suitable ensemble of model options to account for various levels of stock estimate uncertainty. Table 4 provides a description of the alternative model options considered for the sensitivity analysis.

Table 3: Main structural assumptions of the basic model and details of estimated parameters.

Category	Assumptions	Parameters
Recruitment	Occurs at the start of each quarter as 0 age fish. Recruitment is a function of Beverton-Holt stock-recruitment relationship (SRR). Seasonal apportionment of recruitment with temporal deviates 1983 – 2021 Temporal recruitment deviates from SRR, 1983–2021.	R_0 Norm(10,10); $h = 0.80$ $\text{Sigma}R = 0.3.$
Initial population	A function of the equilibrium recruitment in each region assuming population in an initial, unexploited state in 1950.	
Age and growth	8 age-classes, with the last representing a plus group. Growth based on a Richard growth model which approximate the two-stanza growth estimated by Eveson <i>et al</i> (2012). SD of length-at-age based on a coefficient of variation decreasing linearly from 20% at age 0 to 10% at maximum age. Mean weights (W_j) from the weight-length relationship $W = aL^b$.	$L^\infty = 70$ cm, $k = 0.35$, <i>Richard parameter of 2.90.</i> $a = 4.97 \text{ e-}06$, $b = 3.39$
Natural mortality	Constant at 0.8	
Maturity	Length specific logistic function from Grande et al. (2010). Mature population includes both male and female fish (single sex model).	Mat50 38 cm Mat slope -1.25
Selectivity	Cubic spline (7 nodes) selectivity for PL Fishery Cubic spline (5 nodes) selectivity for PSLS and PSFS Fisheries Double normal selectivity for Gillnet, Line, and 'Other' fisheries Logistic selectivity for the longline fishery	
CPUE indices	PL index 1995 – 2022; PSLS index 1990 – 2021. Temporally invariant catchability	
Fishing mortality	Hybrid approach (method 3, see Methot & Wetzel 2013).	
Tagging data	Included only tag release from the RTTP program, and EU PS tag recoveries (adjusted for externally estimated reporting rates); tags assumed to be randomly mixed at the model region four quarters following release;	
Length composition	Multinomial error structure. Length samples assigned maximum ESS of 10.	

Table 4: Description of the sensitivity models for the 2023 assessment. Description of changes are relative to the basic model.

<i>Model</i>	Description
CPUE indices	
<i>PL</i>	Only PL 1995 – 2022 index is included
<i>PSLS</i>	Only PSLS 1991 – 2021 index is included
<i>Behaviour</i>	PSLS 1991 – 2021 index (update to first two quarters of 2021) and the index based on the associative dynamics with floating objects and acoustic 2013 – 2022 are included;
Tagging data	
<i>TagLambda01</i>	Tag lambda = 0.1 for both components of tag likelihood.
<i>exTag</i>	Tagging data excluded
Biological parameters	
<i>Linf</i>	Estimating the L^∞ growth parameter in the model; increase the ESS of longline fishery to 1000
Model structure	
<i>seas</i>	Split the PSFS fishery into four quarterly fisheries and estimate independent selectivity for each quarter; Tagging data excluded
<i>st1980</i>	Starting the model from 1980 assuming a fished equilibrium

4.3 Proposed model ensemble (grid)

On basis of the exploratory analysis, final options were configured to capture the uncertainty related to CPUE indices, stock-recruitment steepness, and growth, which are thought to contribute to the main sources of uncertainty (Table 5). Thus, the final models involved running a full combination of options on CPUE index (2 options), CPUE catchability assumption (2 options), steepness (3 values), growth parameter L^∞ (2 options). The final model grid differs to the options chosen for the 2020 assessment: the suggested model ensemble does not contain the option of an alternative, two-area spatial structure, or the lower tag data weighting option.

Table 5: Description of the final model options for the 2023 assessment. The final models consist of a full combination of options below, with a total of 36 models.

Model options	Description
<i>CPUE option</i>	<ul style="list-style-type: none"> • U1 – PL 1995 – 2022 index is included • Ua – Only PSLS 1991 – 2021 index is included • Ub – PSLS 1991 – 2021 index (update to first two quarters of 2021) and the index based on the associative behavior 2013 – 2022
<i>CPUE catchability</i>	<ul style="list-style-type: none"> • q0 – no annual catchability change • q1– annual catchability increases of 1.25% (both PL and PSLS)
<i>Steepness</i>	<ul style="list-style-type: none"> • h70 – Stock-recruitment steepness parameter 0.7 • h80 – Stock-recruitment steepness parameter 0.8 • h90 – Stock-recruitment steepness parameter 0.9
<i>Growth</i>	<ul style="list-style-type: none"> • L70 – L^∞ parameter fixed at 70 cm as of Eveson et al. 2012 • Linf – L^∞ parameter estimated

5. MODEL RESULTS

5.1 2020 model continuity run

The historical stock estimations from model updates up to 2019 are very comparable to the 2020 assessment reference model (Figure 9), demonstrating the assessment model's relative stability. However, there are significant disparities between 2020 and 2022 when the catches, length compositions, and CPUE are sequentially updated. The stock biomass significantly dropped under the recent catches when there was no updated abundance indicator to inform current recruitment. However, the new CPUE index, notably the PL index, which indicates a strong pulse of recruitment into the fisheries in recent years, is what is driving the substantial increase in biomass between 2020 and 2023. It's important to note that recent compositions of length also seem to indicate above-average recruitment in recent years (Model *2-update-LF* also suggested biomass increased under the current high catches, although to a much lesser extent compared to model *3-update-CPUE*).

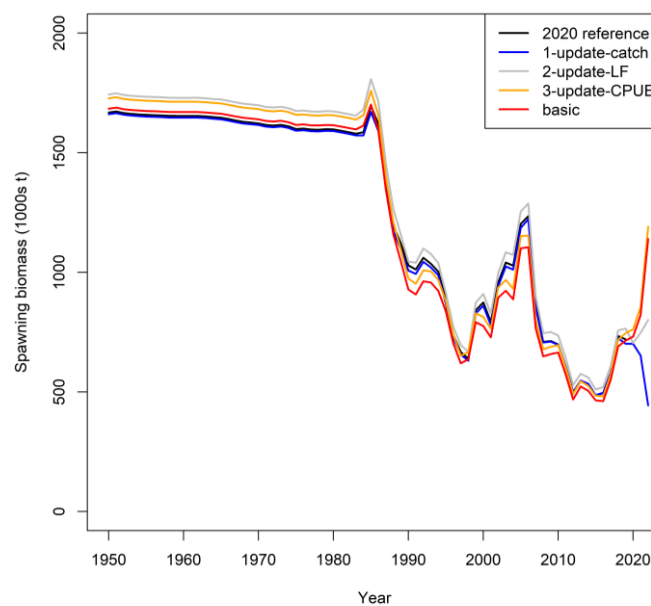


Figure 9: Spawning biomass trajectories for IO skipjack tuna from the stepwise model updates from the 2020 assessment reference model ‘*io_h80_q0_tlambda1*’.

5.2 Basic models

The basic model (see Table 3) extends the definition of F-age for the determination of associated reference points (e.g., FMSY) to be the current model year (i.e., 2022). The summary and diagnostics in this section is largely based on the basic model, but also make references to Model *PL* and *PSLS* (see Table 4), as the latter are the basis for the proposed model ensemble.

5.2.1 Model fits

The basic model included both the Maldives PL index and EU PSLS index (as in the previous assessment) with equal weighting. The two sets of indices are broadly consistent, in view of their overall trend (the increase from 1995 to 2005, the subsequent decline from 2006 to 2015, and the increase in more recent years). The model fitted the PL and PSLS indices reasonably and has broadly captured the inter-annual variability of both time series (Figure 10

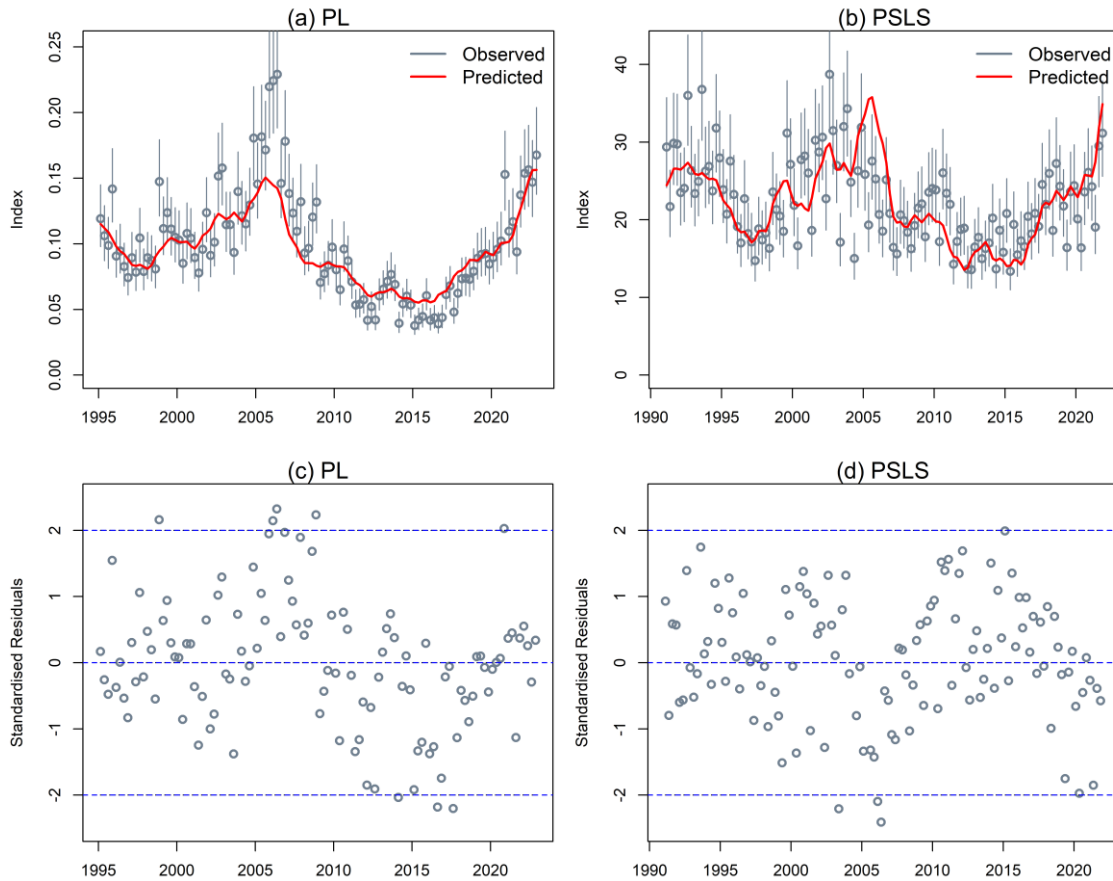


Figure 10). However, there were some misfits in some years reflecting differences in the timing of the peaks in the two CPUE series, and there are also divergent trends in the residuals from the fits (Figure 10), which reflected some of the disagreements between the two series (in terms of the severity of the historical decline and the recent increases). While compromise is expected when fitting multiple abundance indices corresponding to regional fisheries in a spatially aggregated model, it was thought that it would be more appropriate in this case to have separate models based on individual indices independently, each of which would serve as an alternative but equally plausible scenario of historical abundance trend. Figure 11 demonstrates how separate models better capture the uncertainty in stock productivity and trend induced by the various fluctuations in both indices, and how separate models enhance the fits of both the PL and PLS indices.

The fits to the fleet-aggregated length frequency appear generally satisfactory (Figure 12), and the model has captured the gross features of the length composition data (indicating that there is probably no significant bias in the estimates of fishery selectivities). However, there is a lack of fit to the larger fish in the length samples from the longline fishery (see further discussion in Section 5.3), although it is clear that smaller fish were most likely under-sampled. The model has tracked the mean length in the catches reasonably well: it predicted a moderate declining trend for most fisheries which is consistent with the observations (Figure 13). The model does not adequately account for the large inter-annual variability in the PSFS fishery. The length composition from the PSFS fishery shows some seasonal variation as well, with more large fish (>50 cm) in quarters 3 and 4, potentially as a result of seasonal growth or shifts in availability (see further discussions in Section 5.3).

The fit to the observed number of tag recoveries was examined for the fisheries which accounted for most of the tag returns (i.e., PLS). The fit to the number of tag recoveries was examined by recombining the tags into individual release periods (i.e., aggregating the releases by age class) and excluding those recoveries that occurred during the mixing period (Figure 14). The number of tag recoveries varied considerably amongst the release periods and most releases occurred in 2006. Most of the observed tag recoveries in the post mix period were from the PLS fishery and a high proportion

of the total recoveries occurred during the first four quarters following the mixing period. The number of tag recoveries in the first quarter following the mixing period was generally underestimated (Figure 14). This can be an indication that the tags weren't properly mixed with the fish population that was susceptible to the PSLS fishery. Over the longer term, tagged fish were less vulnerable to the purse seine fishery, which resulted in a sharp decline in the number of recoveries. Fits to longer-term recoveries may be also reflecting variable tag reporting or mis-specification of natural mortality.

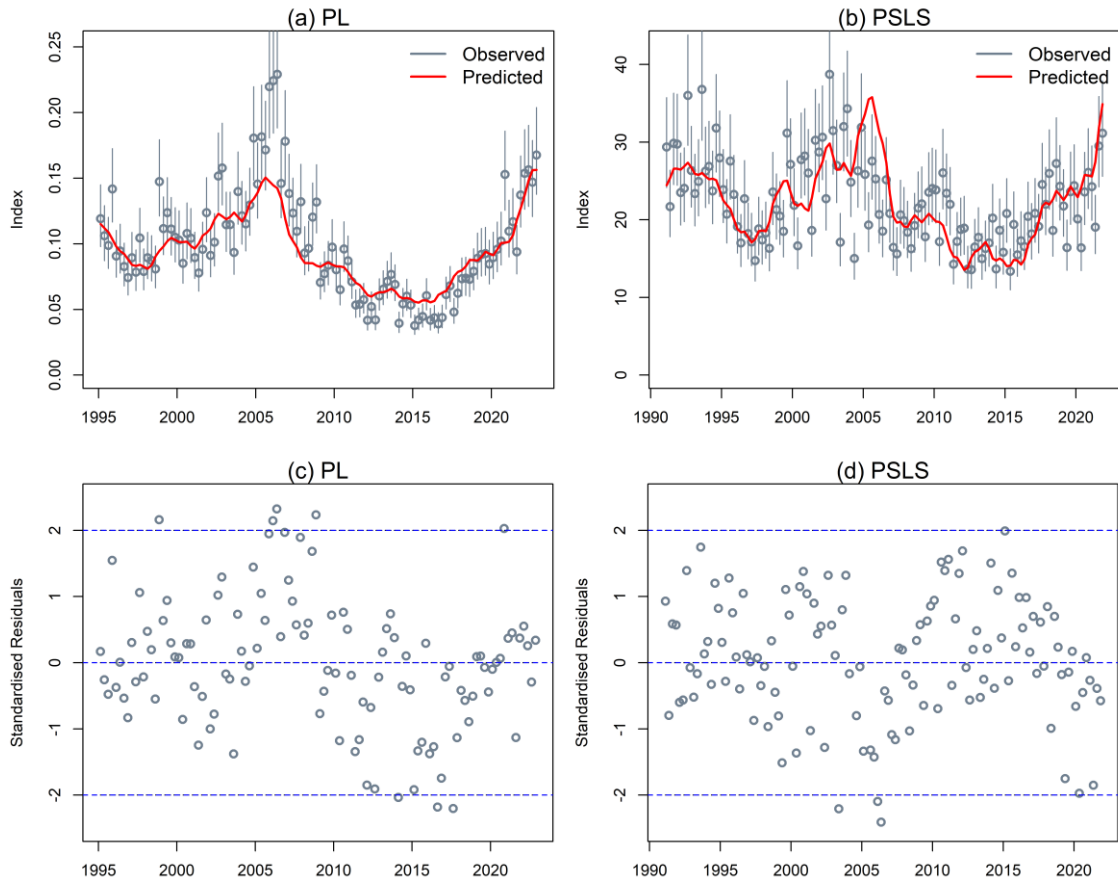


Figure 10: Fits to Maldives PL CPUE 1995 – 2022 (a) and the EU PS CPUE 1991 – 2022 (b) for the basic model. Residuals from the fits are (c) for the PL index and (d) for the PLS index.

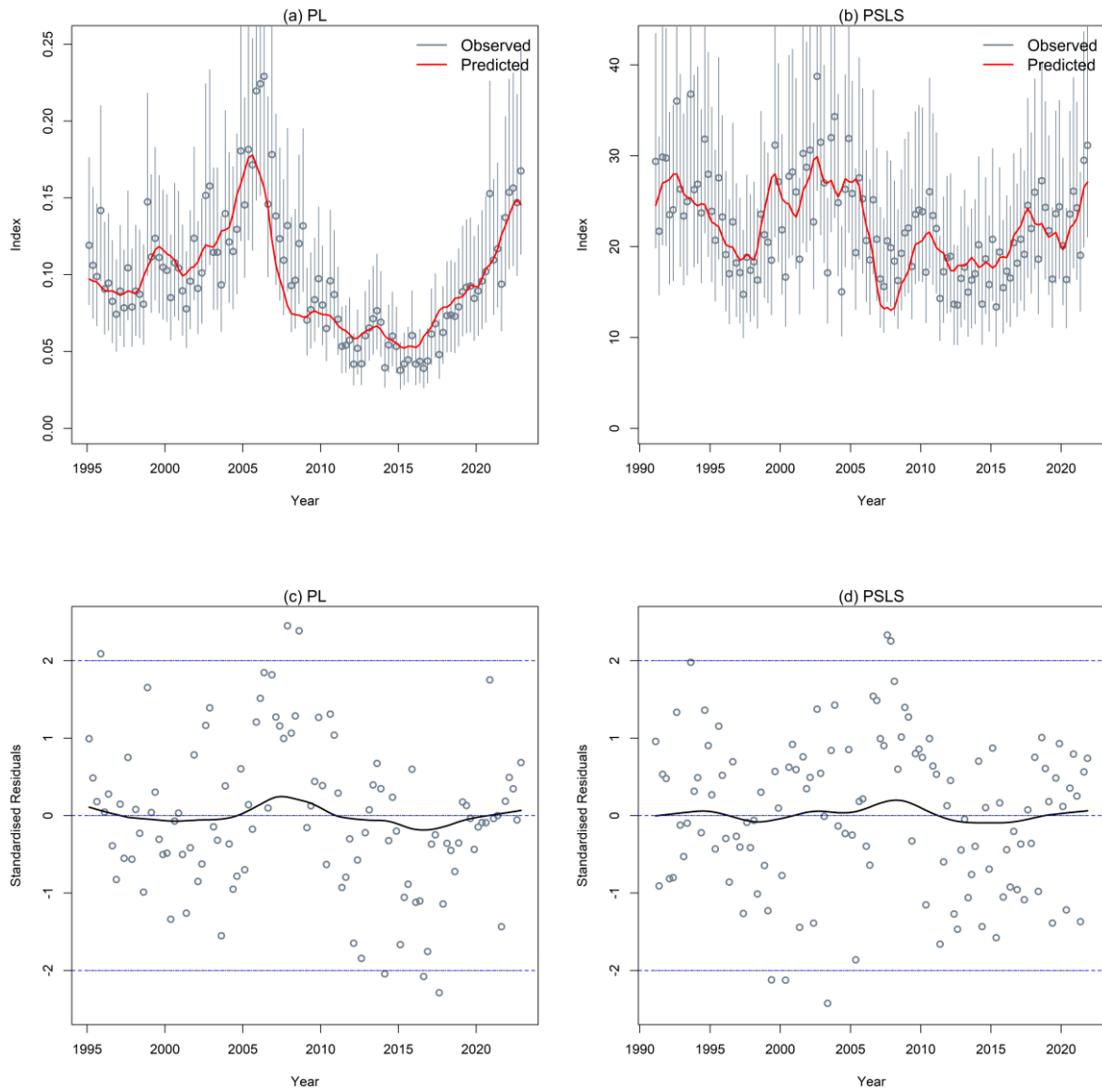


Figure 11: Fits to Maldives PL CPUE 1995 – 2022 (a) for model 'PL', and to the EU PS CPUE 1991 – 2021 for model 'PSLS'; Residuals from the fits are (c) for the PL index and (d) for the PSLs index.

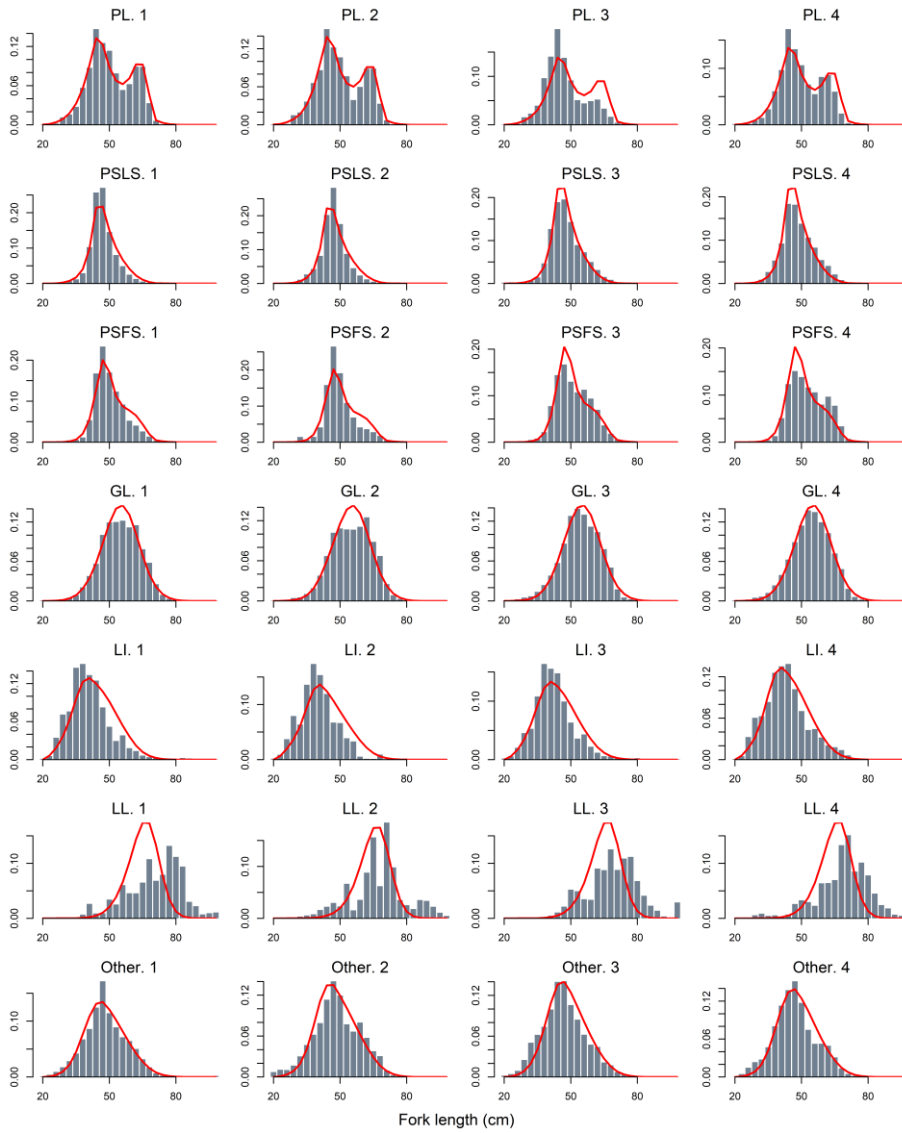


Figure 12: Observed (grey bars) and predicted (red line) length compositions (in 3 cm intervals) for each fishery and season aggregated over years for the basic model.

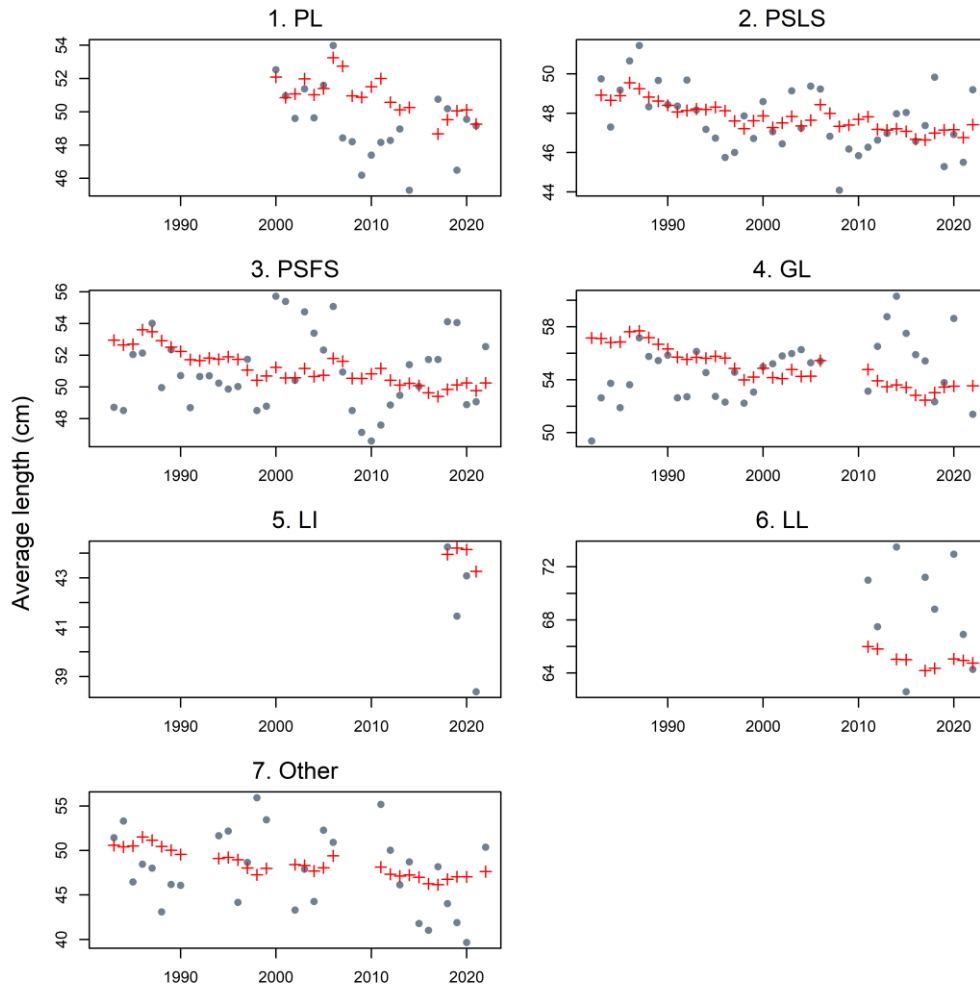


Figure 13: A comparison of the observed (grey points) and predicted (red points and line) average fish length (FL, cm) of skipjack tuna by fishery for the basic model.

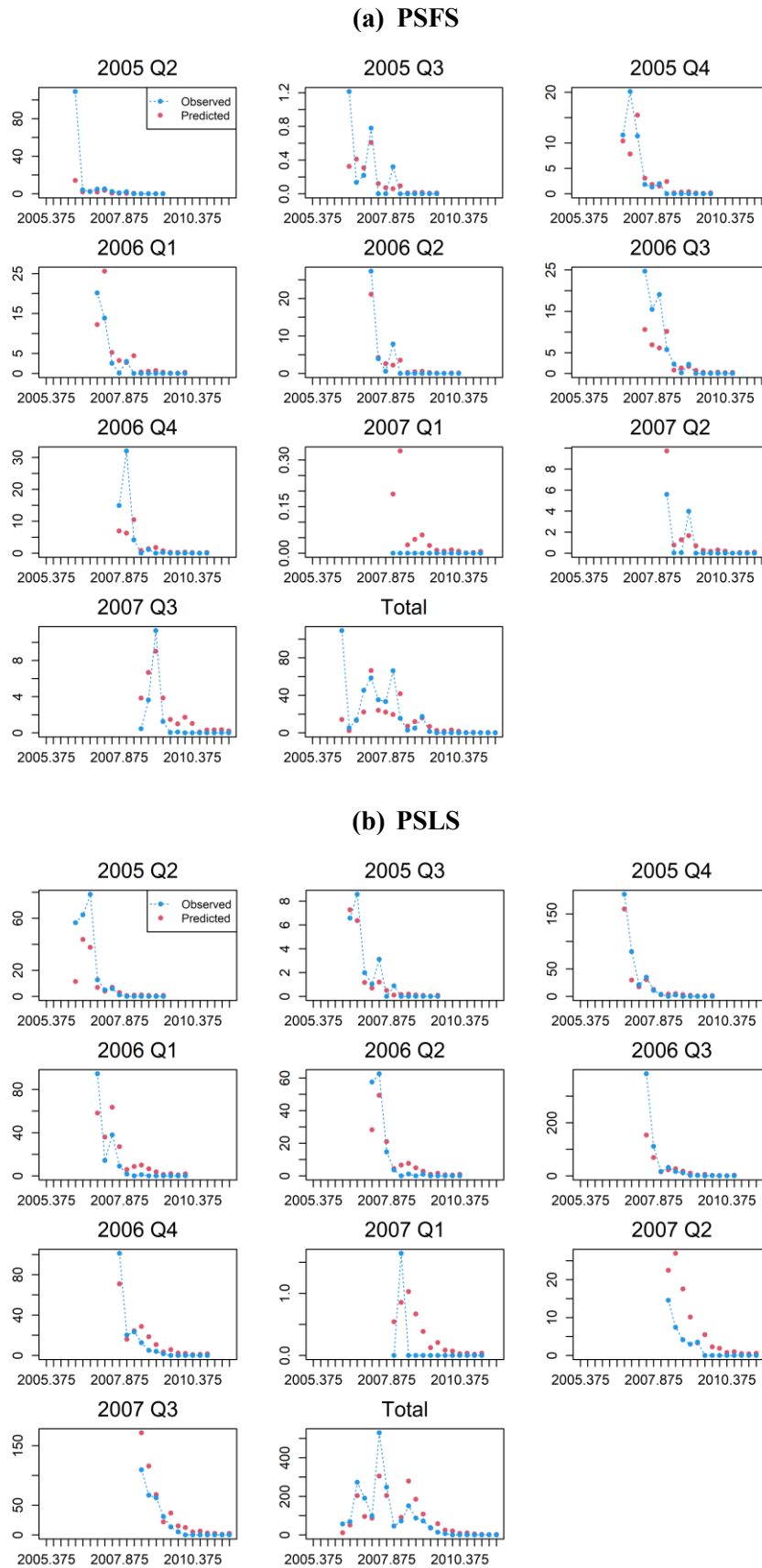


Figure 14: Observed and predicted the number of tag recoveries over time following the mixing period for (a) PSLs and (b) PSFS fishery the basic model. Tag release groups represent the total releases in each quarter (aggregating the age groups that define individual release groups).

5.2.2 Model estimates

The selectivity estimates show that smaller fish (40–60 cm) are caught in the PSLS fishery, whereas larger fish are caught in the GI, LI, and LL fisheries and the youngest ages (including the 38cm maturity threshold) are only weakly vulnerable to the fisheries (Figure 15). The shape of the selectivity for the PL and PSFS reflects the multi-modal length distributions in the fisheries corresponding to a few younger and older age classes. The overall dome-shaped selectivity for most fisheries (except LL) could also be an artefact of the fixed M assumption, combined with the small number of observations of large fish, and uncertain growth curves.

Estimated annual recruitment has a standard deviation of about 0.3, which is commensurate with the assumed value of σ_R . Assuming larger values of σ_R did not change of the pattern nor increase the magnitude of the recruitment deviations, suggesting that the current assumption of σ_R did not impose excessive constraint on estimates of annual recruitment deviations, and that moderate variability is required to match the size composition and CPUE data. The trends in estimated recruitment deviations are very similar between model *PL* and *PSLS*, with periods of low recruitment correspond to the major decline in the PL and PS CPUE indices and recent recruitment has been well above the historical average (Figure 16), driving the increase of the abundance index (model *PSLS* estimated recruitment in 2021 that was 60% above the long-term average, whereas model *PL* estimated that recruitment in 2021 was 95% higher than the average).

The seasonal recruitment distribution estimated by the PL and PSLS models is comparable throughout the four quarters and remarkably constant over time, with season one recruitment estimated to be somewhat higher and season four recruitment to be lower. The seasonal recruiting distribution was mainly driven by seasonal pattern in the CPUE indices.

Estimated biomass showed two steep declines, one in the 1980 through to late 1990s and the other after the mid-2000s (Figure 17), which are explained by a combination of catch removals and recruitment anomalies. The biomass has increased over the last eight years from the historically low level, although the amount of the increase varies depending on which abundance index was employed in the model. It is clear from the stock biomass is strongly driven by recruitment (Figure 18). For both *PL* and *PSLS* models, the deterministic yield curve is well defined, allowing the maximum sustainable yield to be determined (Figure 19). The recruitment variability has a major impact on the surplus production of the stock, which causes the stock trajectory time series to vary significantly from the equilibrium yield curve.

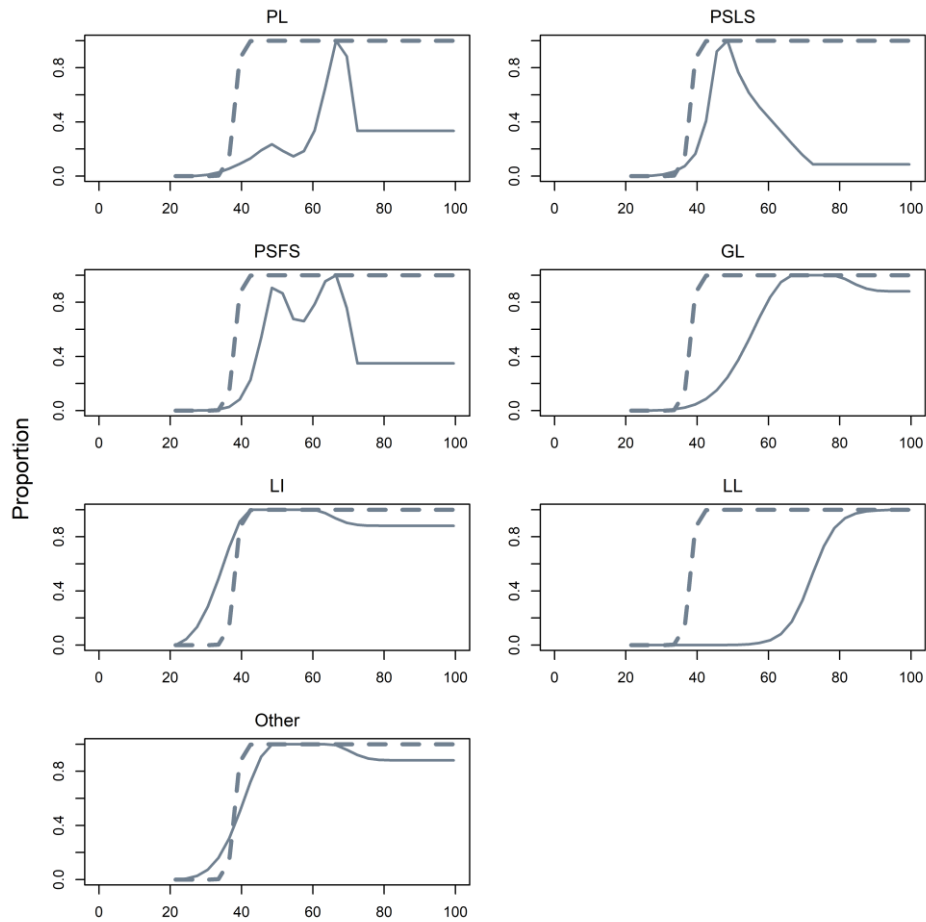


Figure 15: Length-based selectivity estimates by fishery for the basic model (overlaid dashed line is the length-at-maturity).

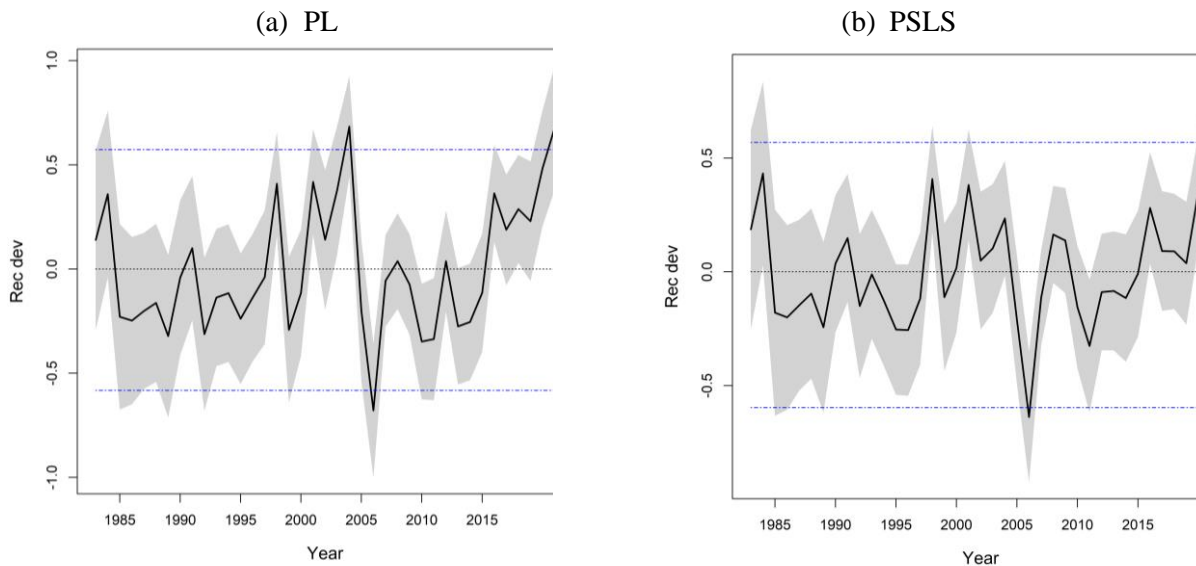


Figure 16: Estimated annual recruitment deviations for (a) model PL and (b) model PSLS. The shaded area represents uncertainty estimates from the MPD fits.

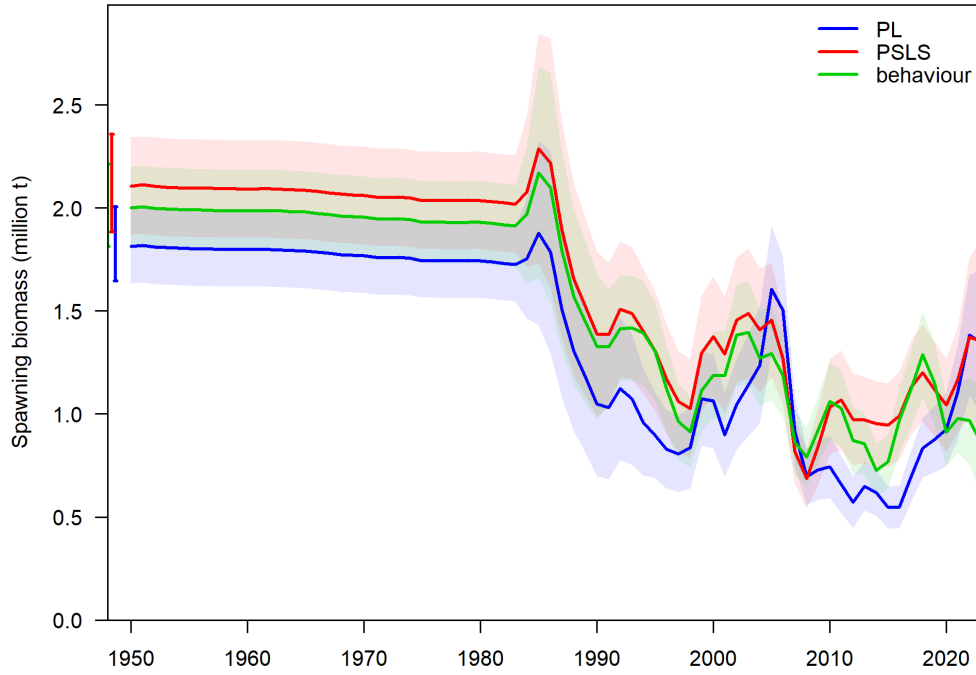
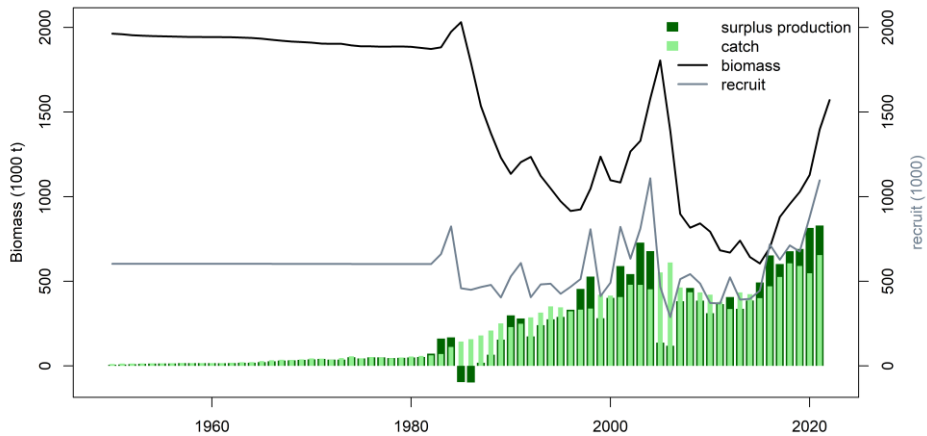


Figure 17: Estimated spawning biomass for model *PL*, *PSLS*, and *behaviour* (see Table 4 for model descriptions).

(a) PL



(b) PSLs

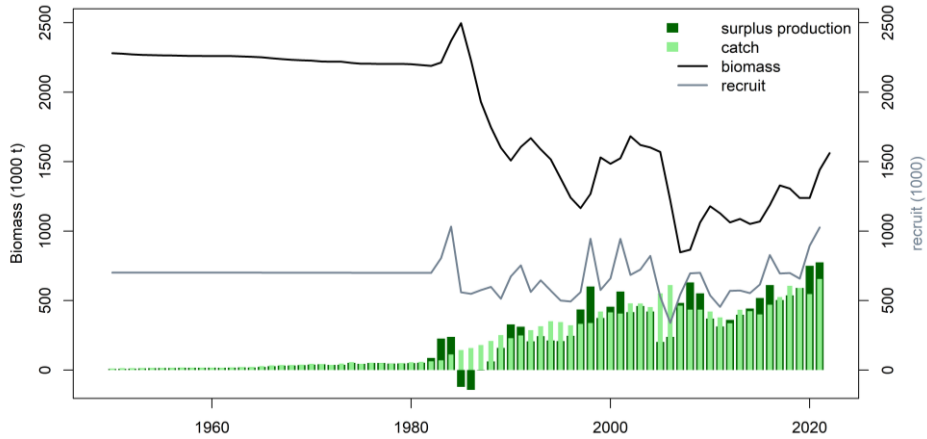


Figure 18:: Estimated annual surplus production, overlaid with catches, biomass, and recruits for model (a) *PL* and (b) *PSLS*.

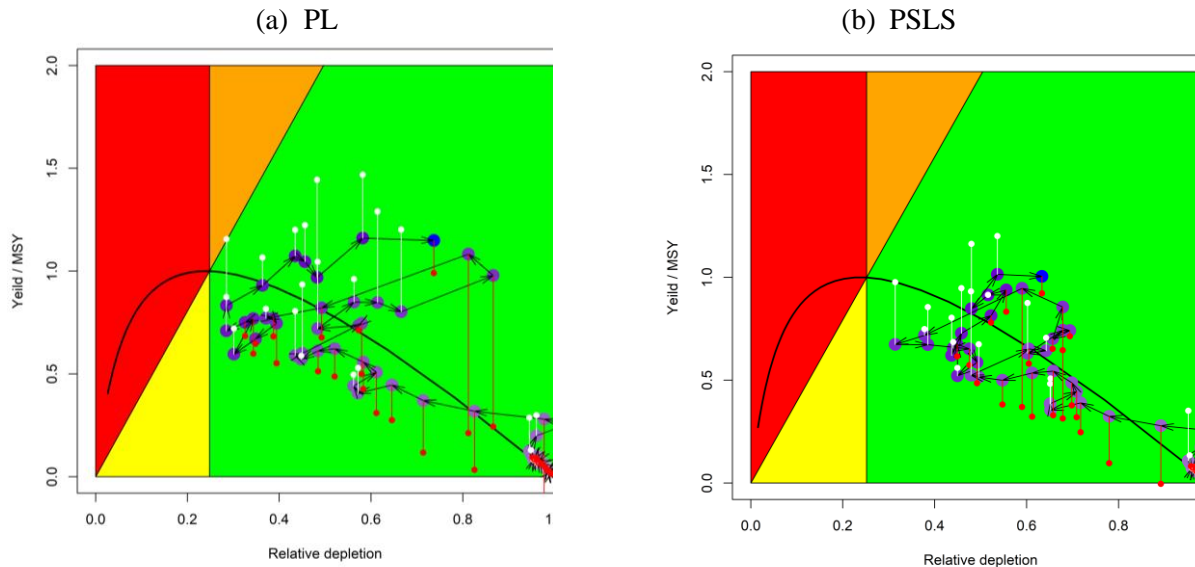


Figure 19: Phase plots of yields (as ratio of MSY) vs. depletion for model (a) PL and (b) PSLs. The parabola curve is the equilibrium yield curve. The purple dots are time series of catch (as ratio of MSY) vs. depletion 1950 – 2022. White and red dots is the actual surplus production in the same year (white indicates the surplus production greater than catch and red indicates lower). The region is partitioned into Kobe quadrats.

5.3 Sensitivity models

Selected results from the sensitivity models are provided in Appendix A. Table A1 summarised the estimates of key model quantities. The estimated SSB_0 ranged from 1,700,000 to 2,300,000 t (Figure A1), and current depletion ranged from 41% to 82% (Table A1).

As demonstrated before, separate model fits to the PL and PSLs index produced stock trend estimates that are more consistent with the respective index, and the PL index model estimated a more optimistic level of current depletion. Alternatively model *behaviour* included both the PSLs index and the behavior-based index (the behaviour-based series are too short to be a stand-alone index, but this model removed the very high index in the last two quarters of the PSLs series to alleviate the conflict between the two series), which estimated a significantly lower level of current depletion than the model based solely on the PSLs index.

The longline fishery has extremely low catches of skipjack tuna, but they are included to provide size-based information. The LL fishery caught mostly large skipjack tuna and the right-hand side of the LL length distribution appeared to be poorly fitted (see Figure 12). The LL catches of skipjack tuna is negligible and any bias in the LL selectivity is not expected to have any noticeable impact on the model. However, the lack of fits to the larger size classes may indicate that the assumed growth is probably biased. Model *Lin* estimated the L^∞ as a free parameter (to do that the model also increased the sample size of the longline length composition data). The L^∞ parameter was estimated to be about 88 cm (about 18 cm higher than the estimate of Evenson et al. 2012), which allowed the model to better explain the larger fish in the LL length samples (Figure A2). The model estimated a more depleted current stock status (41% B_0) as a higher L^∞ implied that there had been more large fish in the unfished population. Although lower values of L^∞ was estimated across the proposed model ensemble (ranging from 79 to 81 cm, see section 5.4), they are still much higher than the estimate of Evenson et al. 2012.

A seasonally structured fishery where selectivity is independently estimated for each quarter can better account for the variability in the length distribution of the PSFS fishery (Figure A3). Model *seas* estimated a significant difference in selectivity between the first two and last two quarters, and there is a shift towards the selection of larger fish in the second half of the year. The use of seasonal selectivity in this fishery appears to have little impact on overall estimates of stock abundance because the catch

from the PSFS fishery is very small.

There is conflict between the tag release/recovery data and the CPUE data, and the relative weighting of each dataset influences the population scale parameter (R_0). Downweighting the tag data yielded substantially higher level of stock biomass and MSY (Table A1). Reducing the weight of tag data (via the lambda multiplier of the likelihood component) to 10% has a similar effect to a model that excluded the tagging data. A likelihood profile analysis may provide further insights into the conflict between the CPUE and tag data.

5.4 Proposed model ensemble

Despite of the overall consistency between the PL and PSLs index, they differed in the extent of implied stock productivity (e.g., B_0) and depletion, with the PL index representing a larger decline in vulnerable abundance since mid-2000 but a more significant increase from 2016 – 2022. The index based on the associative dynamics with floating objects corroborate the increasing trend in the PSLs index from 2015 to 2018, but showed an opposite trend from 2018 – 2022, with a large decline in the latter years. There has also been some concern about the reliability of abundance indices produced from the purse seine fishery, it is important to account for these alternate abundance trend scenarios in the model ensemble.

The WPTT22 in 2020 suggested including catchability trends of 0 and/or 1.25% per year in the final model grid for the PSLs index, based on a proof-of-concept analysis that assessed PS catchability changes using bigeye and yellowfin tuna assessments (IOTC 2020). Given the technological advancements that are well known to have happened in the fisheries and the resulting increased fishing efficiency, the WPTT22 also advised applying the catchability changes to the Maldives PL index.

It is also suggested to include the scenarios where the L^∞ parameter is freely estimated within the model (and increasing the sample size of the LL length composition data) given the uncertainty associated with growth parameters as evident in the poor model fits to the longline length composition.

The proposed model options also included three alternative values of steepness of the BH SRR (h 0.7, 0.8 and 0.9). These values are considered to encompass the plausible range of steepness values for skipjack tuna.

Synthesizing above, the proposed model ensemble corresponds to a full combination of three CPUE options, two catchability trend scenarios, three steepness values, and two growth parameter options, with a total of 36 models (see Table 5). These models encompass a wide range of stock trajectories (Figure 20). Across the model ensemble, initial spawning biomass (SB_0) ranged from 1 826 990 t to 2 494 210 t, current depletion ranged from 36% to 74% (SSB_{2022}/SSB_0) (Table 6 and Figure 20). L^∞ was estimated for half of the models in the ensemble, ranging from 79 to 81 cm. In general, high steepness, the PL index, and fixed L^∞ are associated with lower SB_0 and higher current stock status (depletion), whereas low steepness, the behaviours and the PSLs index, free L^∞ option, are typically associated with high SB_0 and lower current stock status (Table 6). As expected, the assumption of increasing catchability overtime also resulted in lower estimates of the current stock depletion.

Table 6: Maximum Posterior Density (MPD) estimates of the main stock status indicators from individual models from final model options.

	SB_0	SB_{MSY}	SB_{2022}	SB_{2022}/SB_0	SB_{2022}/SB_{MSY}	F_{2022}/F_{MSY}	$F_{40\%SB}$	F_{MSY}	MSY	$Max\ grad$
io_h70_U1_q0_L70	1 956 540	547 916	1 453 510	0.74	2.65	0.48	0.55	0.81	521 849	0.00053
io_h70_U1_q0_Linf	2 339 430	658 645	1 306 350	0.56	1.98	0.65	0.46	0.69	485 130	0.00210
io_h70_U1_q1_L70	2 003 620	561 136	1 312 620	0.66	2.34	0.53	0.55	0.81	534 009	0.00003
io_h70_U1_q1_Linf	2 40 9610	678 643	1 143330	0.47	1.68	0.74	0.46	0.69	499 321	0.00048
io_h70_Ua_q0_L70	2 228 800	621 379	1 403 300	0.63	2.26	0.50	0.54	0.80	585 842	0.00010
io_h70_Ua_q0_Linf	2 494 210	701 165	1 369 270	0.55	1.95	0.60	0.48	0.71	535 164	0.00009
io_h70_Ua_q1_L70	2 293 910	639 860	1 224 510	0.53	1.91	0.57	0.54	0.80	603 143	0.00003
io_h70_Ua_q1_Linf	2 575 490	724 391	1 123 150	0.44	1.55	0.73	0.47	0.71	551 499	0.00011
io_h70_Ub_q0_L70	2 155 140	600 518	1 084 760	0.50	1.81	0.65	0.54	0.80	566 358	0.00004
io_h70_Ub_q0_Linf	2 395 580	673 029	1 005 350	0.42	1.49	0.82	0.48	0.71	515 189	0.00035
io_h70_Ub_q1_L70	2 223 240	619 821	987 715	0.44	1.59	0.71	0.54	0.80	584 455	0.00008
io_h70_Ub_q1_Linf	2 485 230	698 480	869 198	0.35	1.24	0.94	0.48	0.71	533 129	0.00064
io_h80_U1_q0_L70	1 826 990	437 787	1 393 910	0.76	3.18	0.38	0.61	1.05	560 600	0.00009
io_h80_U1_q0_Linf	2 146 560	519 452	1 232 100	0.57	2.37	0.52	0.51	0.91	510 709	0.00065
io_h80_U1_q1_L70	1 869 290	448 055	1 252 150	0.67	2.79	0.42	0.61	1.05	573 278	0.00000
io_h80_U1_q1_Linf	2 209 420	535 040	1 067 650	0.48	2.00	0.60	0.51	0.90	525 233	0.00088
io_h80_Ua_q0_L70	2 121 290	505 021	1 377 500	0.65	2.73	0.39	0.60	1.04	641 512	0.00008
io_h80_Ua_q0_Linf	2 344 650	566 044	1 329 570	0.57	2.35	0.47	0.52	0.93	577 874	0.00003
io_h80_Ua_q1_L70	2 182 590	520 149	1 203 870	0.55	2.31	0.45	0.60	1.04	660 308	0.00035
io_h80_Ua_q1_Linf	2 419 580	584 759	1 090 350	0.45	1.86	0.57	0.52	0.93	595 181	0.00011
io_h80_Ub_q0_L70	2 051 060	488 064	1 067 550	0.52	2.19	0.51	0.60	1.04	620 349	0.00013
io_h80_Ub_q0_Linf	2 245 850	541 942	971 641	0.43	1.79	0.64	0.53	0.93	554 983	0.00238
io_h80_Ub_q1_L70	2 114 620	503 715	973 243	0.46	1.93	0.55	0.60	1.04	639 847	0.00001
io_h80_Ub_q1_Linf	2 329 300	562 599	841 019	0.36	1.49	0.74	0.52	0.93	574 250	0.00018

	<i>SB₀</i>	<i>SB_{MSY}</i>	<i>SB₂₀₂₂</i>	<i>SB₂₀₂₂/SB₀</i>	<i>SB₂₀₂₂/SB_{MSY}</i>	<i>F₂₀₂₂/F_{MSY}</i>	<i>F_{40%SB}</i>	<i>F_{MSY}</i>	<i>MSY</i>	<i>Max grad</i>
io_h90_U1_q0_L70	2 243 070	434 653	1 305 060	0.58	3.00	0.35	0.57	1.28	630 177	0.00002
io_h90_U1_q0_Linf	2 106 230	396 125	1 191 810	0.57	3.01	0.33	0.64	1.43	728 398	0.00120
io_h90_U1_q1_L70	2 313 580	449 361	1 072 110	0.46	2.39	0.42	0.57	1.28	648 661	0.00007
io_h90_U1_q1_Linf	1 979 980	371 473	1 057 620	0.53	2.85	0.37	0.64	1.43	684 778	0.00034
io_h90_Ua_q0_L70	2 144 490	415 543	951 836	0.44	2.29	0.47	0.57	1.29	604 187	0.00009
io_h90_Ua_q0_Linf	2 040 080	383 563	965 943	0.47	2.52	0.41	0.64	1.43	705 790	0.00009
io_h90_Ua_q1_L70	2 223 470	431 785	826 690	0.37	1.91	0.54	0.57	1.28	624 958	0.00009
io_h90_Ua_q1_Linf	2 243 070	434 653	1 305060	0.58	3.00	0.35	0.57	1.28	630 177	0.00000

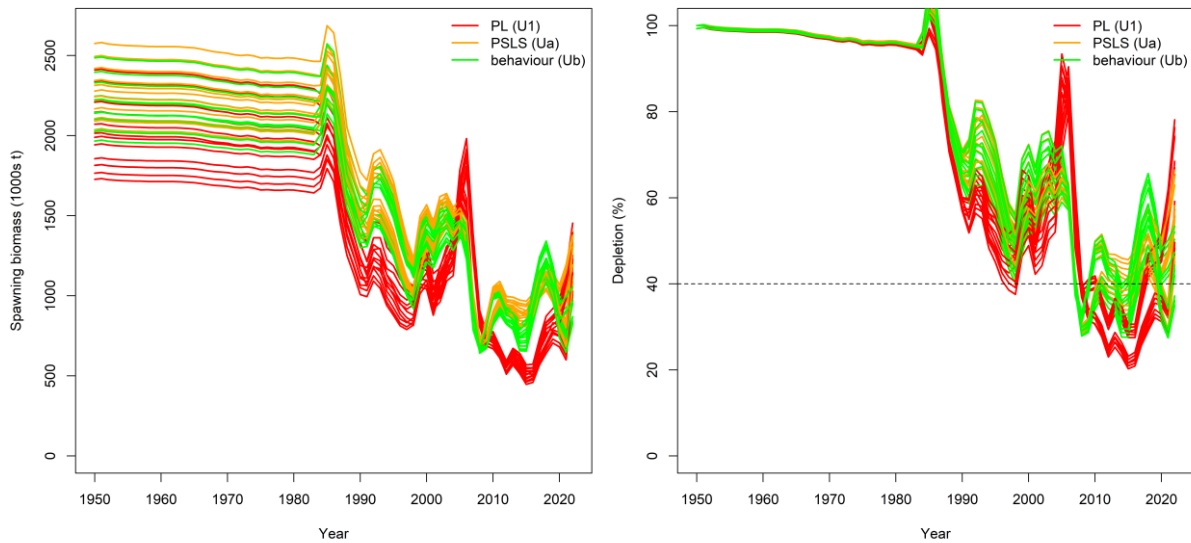


Figure 20: Spawning biomass trajectories from the proposed model ensemble (details in Table 5)

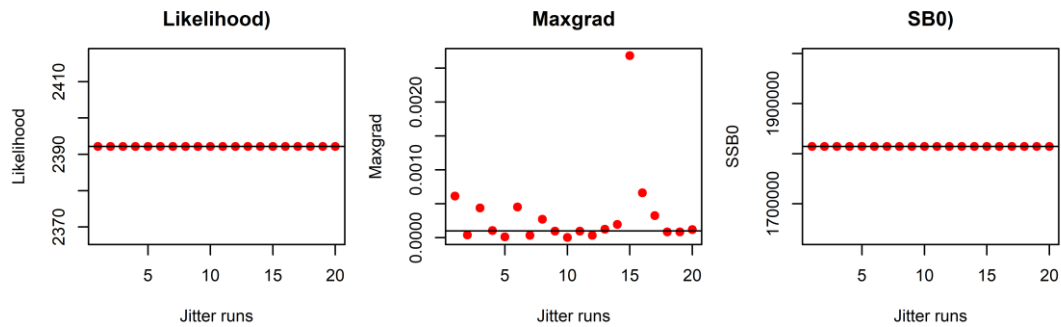
5.5 Diagnostics

Several diagnostic tools were run for the *PL* and *PSLS* model, including Jittering, likelihood profiling, and retrospective analysis.

5.5.1 Jitter analysing

Jittering involves running the model using different initial values of the estimated parameters (adding random error to the initial values) and comparing the final values of the objective function negative (negative likelihood). It provides an effective way to test whether model estimates converge to a (relative) global minimum. Twenty jitter analyzes were performed on the *PL* and *PSLS* models and there was no indication that the models converged to a local minimum (as shown by the same likelihood values and estimated SB0). Interestingly, the final gradient values fluctuated across runs, many of them exceeding the convergence threshold (set at 0.0001), possibly because the model converged to a region close to the minimum which include different gradients. This suggests that the final convergence value itself may not be a good indicator of model convergence, whereas the Jittering of the objective function values is more useful.

(a) PL



(b) PSLS

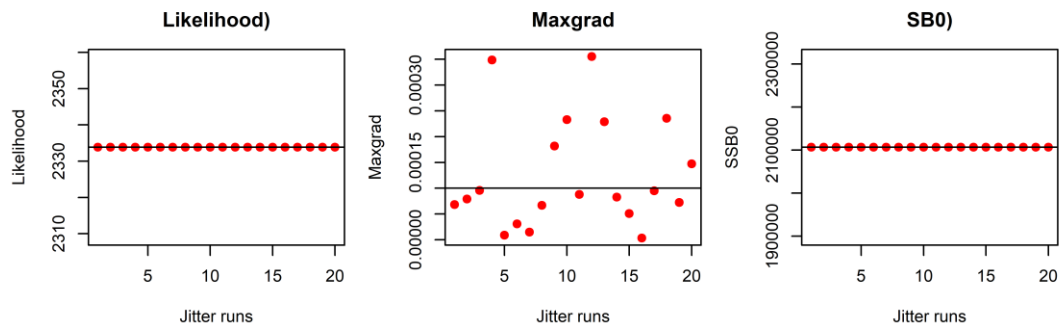


Figure 21: Jittering analysis performed to the PL and PSLS model, showing the final objective function values, gradient, and estimate of SB0 obtained by running the model from different parameter starting values (n=20).

5.5.2 Profile likelihood

The profile likelihood on R_0 confirmed that the (relative) global minimum was obtained by the maximum likelihood estimate for both the *PL* and *PSLS* models (Figure 22). For the *PL* model, there are conflicts between the PL index, size frequency, and tagging data, where the size data appears to support a higher R_0 , the PL index favours a low R_0 , and tag data supports an even lower R_0 ; for the *PSLS* model, the tag data supports a lower R_0 , but there is more consistency between the PSLS index and size data, both supporting a higher R_0 . Further breakdown of the likelihood components suggested that the length composition from the main fisheries (i.e., PL and PSLS) appears to be consistent with the total likelihood, providing both the upper and lower bounds for R_0 , whereas fisheries that caught mostly large fish (i.e. LL, GI, LI) provide no constrain on the upper bound for R_0 (Figure 23). The average fish length in the PL and PSLS fisheries shows a declining trend whereas it remains relatively stable in the GI fisheries (see Figure 13). Nonetheless, under the current weighting (i.e., effective sample size), the overall influence of the length composition on the stock estimates appears small.

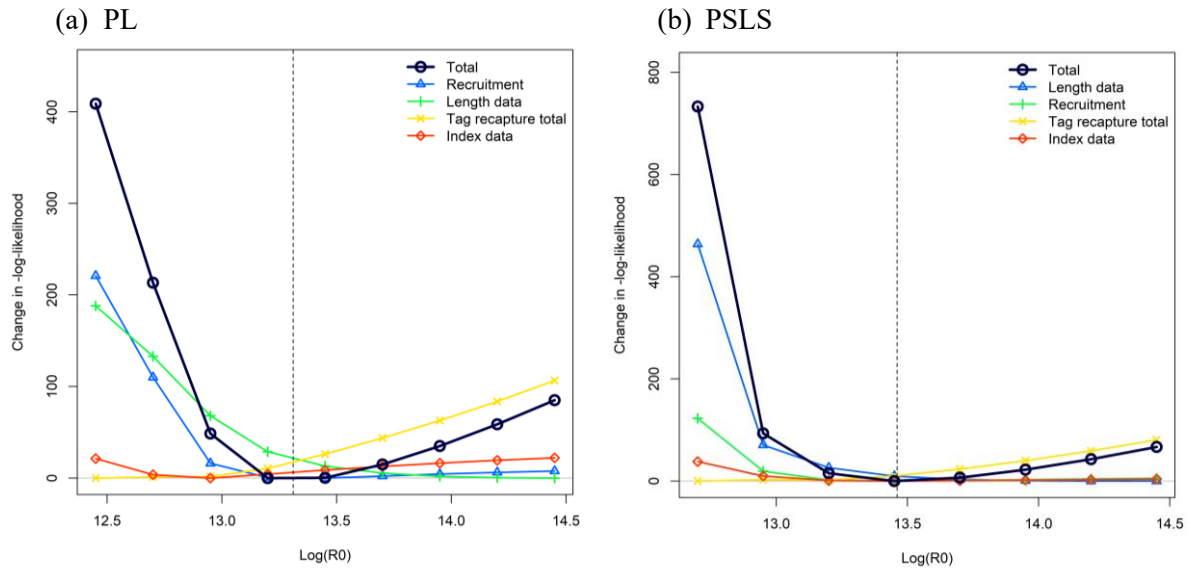


Figure 22: Likelihood profile for the *PL* model (left) and *PSLS* model (right).

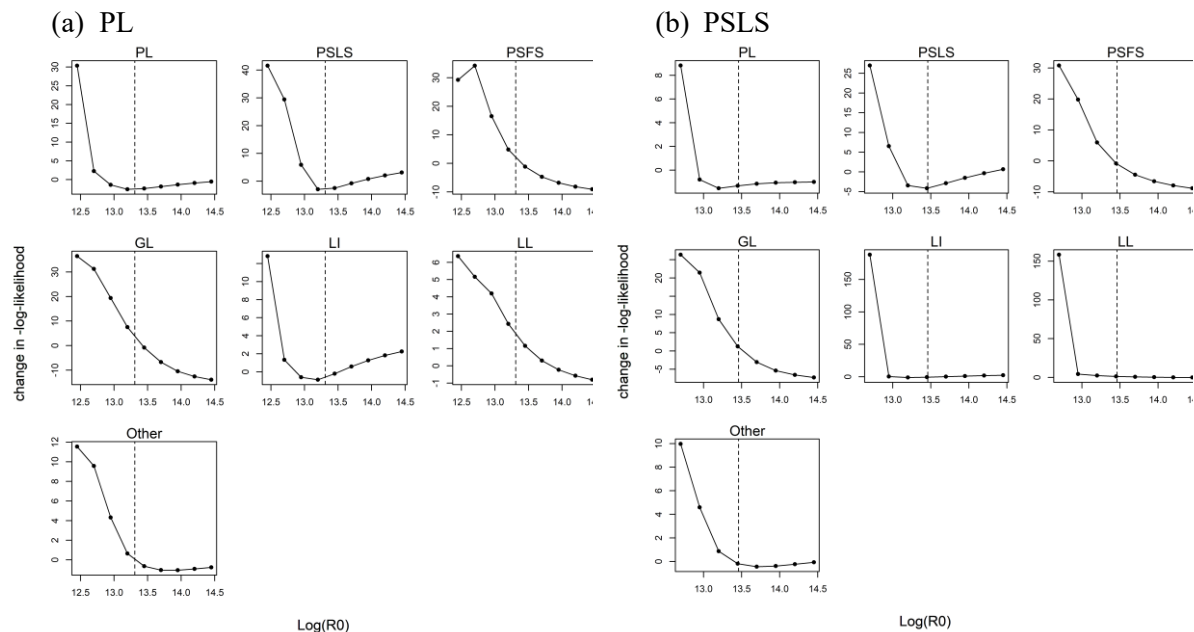


Figure 23: Component likelihood profile from the length composition data for the *PL* model (left) and *PSLS* model (right).

5.5.3 Retrospective analysis

Retrospective analysis is a diagnostic approach to evaluate the reliability of parameter and reference point estimates and to reveal systematic bias in the model estimation. It involves fitting a stock assessment model to the full dataset. The same model is then fitted to truncated datasets where the data for the most recent years are sequentially removed. The retrospective analysis was conducted to both *PL* and *PSLS* models for the last four years of the assessment time horizon to evaluate whether there were any strong changes in results. The analysis indicated that there is only a very minor retrospective pattern for the virgin biomass estimate (e.g., reduced SB as data was sequentially removed), but biomass estimates since 1985 are very consistent with respect of the recent data. Overall, the retrospective pattern appears insignificant (with Mohn’s ϕ for SB ≈ -0.05), which provided some confidence on the robustness of the models.

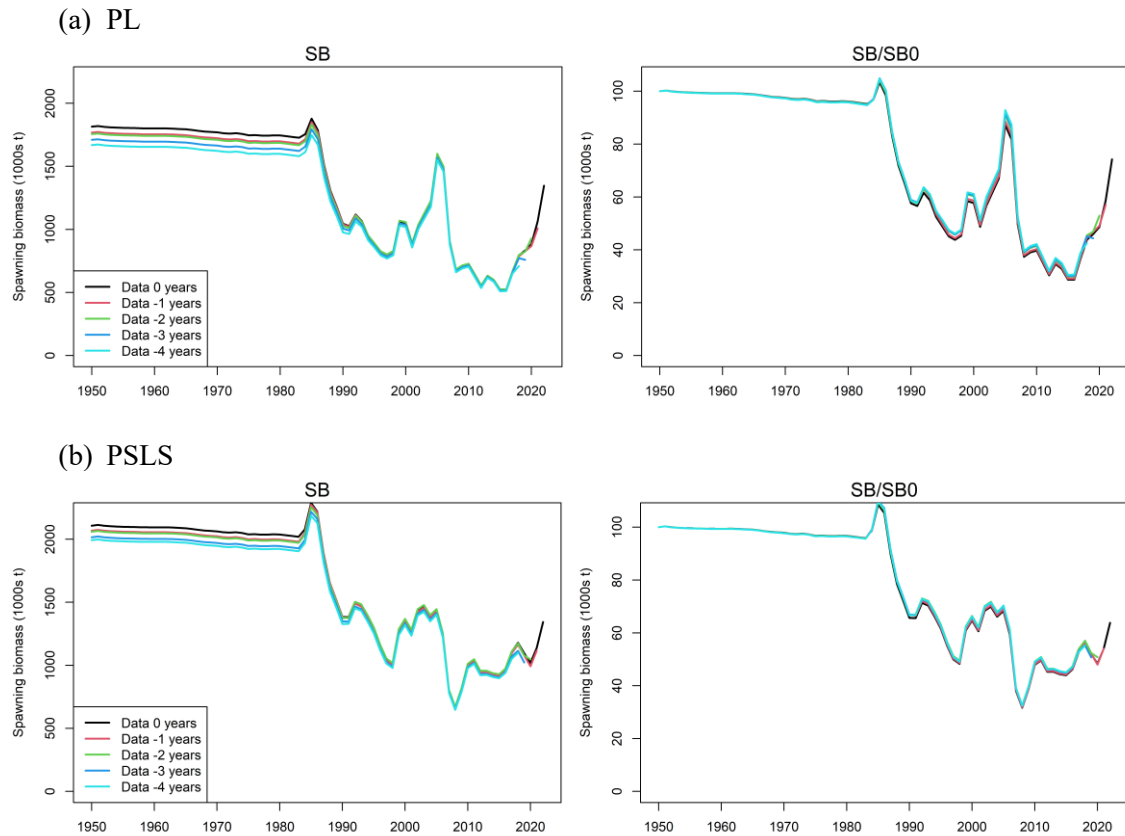


Figure 24: Retrospective analysis summary for the basic model. Each panel shows estimates of key indicators from models with data sequentially removed for 1 – 4 years.

6. STOCK STATUS

6.1 Current status and yields

Estimates of stock status were determined from the model ensemble, which has included alternative options on CPUE indices, alternative assumptions on catchability, and alternative values of SRR steepness and growth. Stock status was determined for individual models (Table 6), as well as for all (36) models combined, incorporating uncertainty of each model based on estimated variance-covariance matrix of parameters (Table 7).

MSY-based reference points (see Section 3.5) were derived based on the average F-at-age matrix in 2022, representing the most recent pattern of exploitation from the fishery. For the selected model options, point estimates of *MSY* ranged from 485 000 t to 728 000 t (Table 6). Annual catches over the last five years have been within the range of the estimated target yield (Figure 25). Models with higher steepness generally yielded comparatively higher estimates of optimal yield.

In general, current stock biomass relative to the *MSY*-based benchmarks are not fundamentally different for the range of model options. Averaging across the model grid, fishing mortality rates have been increasing significantly since 1980, and has decreased rapidly since 2016, despite that catches have peaked at historical high levels over the last few years (Figure 25). Biomass was estimated to have declined considerably in the 1980s, again in the mid-2000s, but have increased rapidly since 2015 (Figure 25).

Estimates were combined across from the 36 models to generate the KOBE stock status plot (Figure 26). For individual models, the uncertainty is characterised using the multivariate lognormal Monte-Carlo approach (Walter & Winker 2019, Winker et al. 2019), based on the maximum likelihood

estimates and variance-covariance of F/F_{MSY} and SB/SB_{MSY} . Thus, estimates of stock status included both within and across model uncertainty. Combined across the model ensemble, SB_{2022} was estimated to be of 2.30 SSB_{MSY} (1.57– 3.40), and F_{2022} was estimated 0.49 F_{MSY} (0.32–0.75). Current depletion, SB_{2022}/SB_0 was estimated to be about 53% (42%-68%), which is also above the target level of 40% specified in the HCR (res. 16/02). The probability of the stock being in the green Kobe quadrant in 2023 is estimated to be about 98%. The stock is therefore considered not to be overfished and is not subject to overfishing in 2022. While all models in the grid has estimated that the stock is located in green Kobe quadrat, models assuming high steepness, fixed L^∞ , PL index, and constant catchability led to estimates of higher current status and lower fishing pressure, and models assuming low steepness, higher L^∞ (estimated), PLS and behaviour based indices, and increased catchability led to estimates of lower current status and higher fishing pressure (**Figure 27**).

Table 7: Estimated Status of skipjack tuna in the Indian Ocean from the model ensemble.

Catch in 2022:	648 695
Average catch 2018–2022:	601 499
MSY (1000t) (80% CI)	584 774 (512 228–686 071)
F_{MSY}	0.99 (0.71–1.42)
$F_{40\%SSB}$	0.55 (0.48–0.65)
SB_0 (1000 t) (80% CI):	2 177 144 (1 869 035–2 465 671)
SB_{2022} (1000 t) (80% CI):	1 142 919 (842 723–1 461 772)
SB_{MSY}	513 831 (369187–678936)
SB_{2022}/SB_0 (80% CI):	0.53 (0.42–0.68)
SB_{2022} / SB_{MSY}	2.30 (1.57–3.40)
F_{2022} / F_{MSY}	0.49 (0.32–0.75)

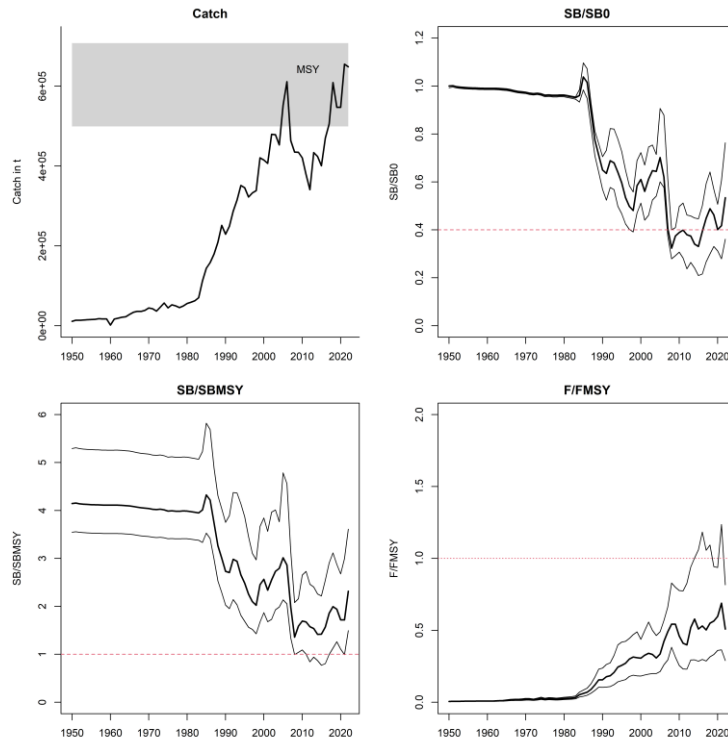


Figure 25: Estimated stock trajectories for the Indian Ocean skipjack from the final model grid. Thin black lines represent 5%, 50%, 95% percentiles. In the catch plot, dotted lines represent estimate of $Yield_{40\%SSB}$, the shaded area represents 5th and 95th percentiles.

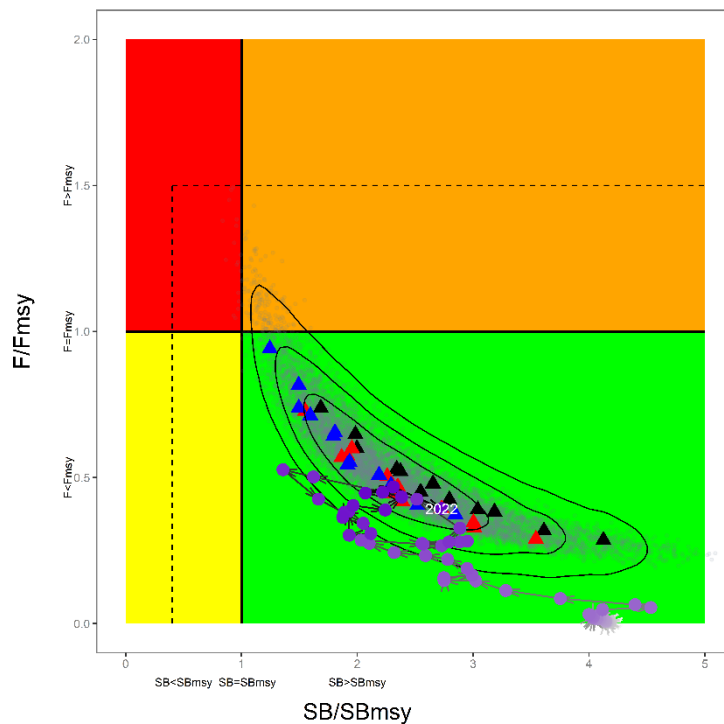


Figure 26: current stock status, relative to SB_{MSY} (x-axis) and F_{MSY} (y-axis) reference points for the final model grid. Triangles represent MPD estimates from individual models (black, models based on PL index; red, models based on PL index; blue, models based on and both PSLs and behaviour index). Grey dots represent uncertainty from individual models. The arrowed line represents time series of historical stock trajectory for model *PSLS*. The dashed lines represent limit reference points for IO skipjack ($SB_{lim} = 0.4SB_{MSY}$; $F_{lim} = 1.5F_{MSY}$). Contours represents 50, 80, and 90% confidence region.

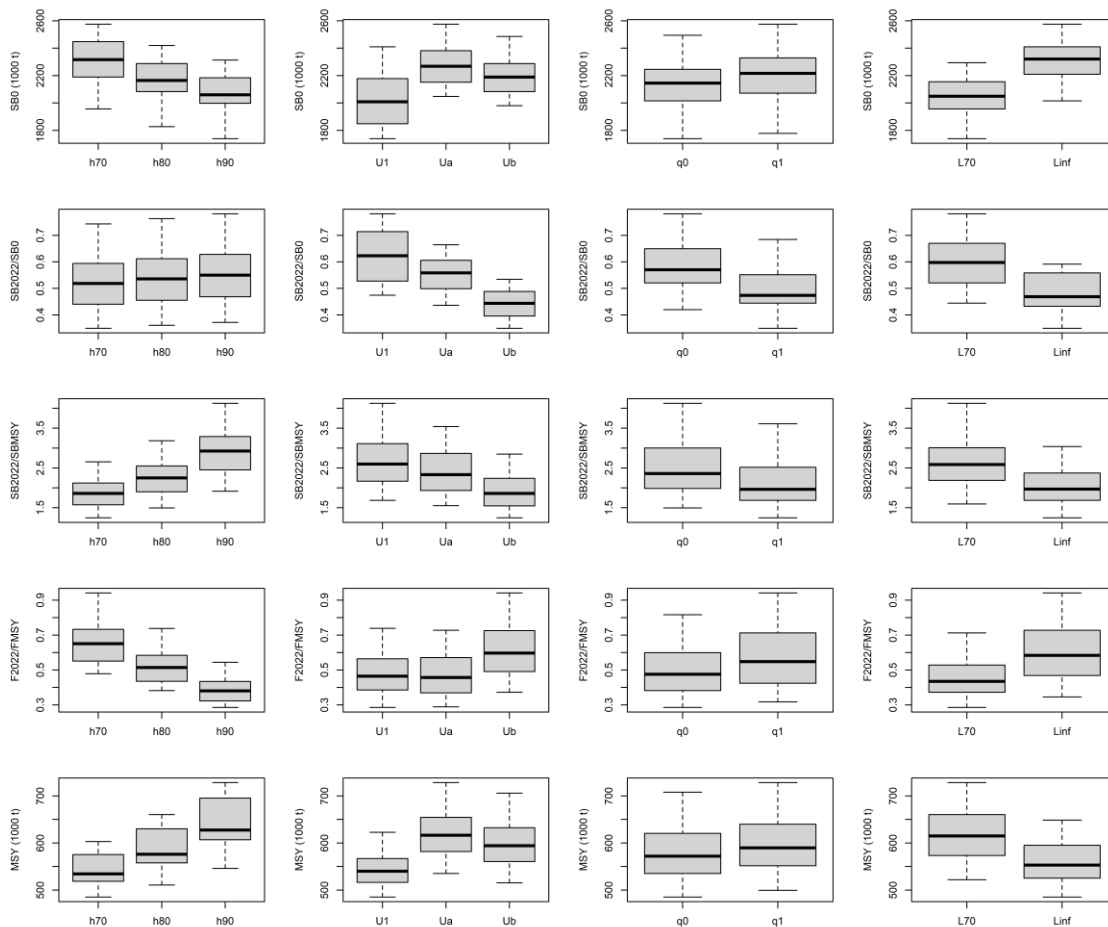


Figure 27: range distribution of key reference quantities (SB_0 , SB/SB_0 , SB/SB_{MSY} , and MSY) across models in the final ensemble by uncertainty axis.

7. DISCUSSION

This report presents a stock assessment for Indian Ocean skipjack using a sex-aggregated, age-structured Stock Synthesis model. It represents an update and revision of the 2020 assessment model with newly available information, including updated and revised CPUE indices and length composition data. There are no fundamental changes to the structure of the model compared to the previous assessment (Fu 2020), with the revisions mostly concerning the refinement of the fleet compositions. A range of sensitivity models were explored to assess the impact of key data sets and model assumptions. The final model options involved running a combination of configuration and model settings related to the CPUE options, catchability assumptions, stock-recruitment steepness, and growth. These model options are thought to have contributed to the main source of uncertainty associated with estimates of stock dynamics and productivity. The final estimates of stock status are based on a model grid of 36 models, incorporating uncertainty estimates from both within and across the model ensemble. Considering the quantified uncertainty, spawning stock biomass in 2022 was estimated to be 53% of the unfished levels ($SB_{2022}/SSB_{MSY} = 2.30$). Current fishing mortality was estimated to be lower than the target fishing mortality ($F_{2022}/F_{MSY} = 0.49$). The overall estimates indicate that the condition of the stock has significantly improved since the assessment.

There has been a substantial increase of fishery dependent abundance index in recent years: the CPUE from the Pole and line fishery increased by 75% from 2019 to 2022, and the PSLs also increased by over 30% between 2019 and 2021. As the overall catches for skipjack have been remaining high, the increase in abundance was driven by an increase in recruitment which was estimated to be much above the long-term average. Environmental conditions (such as sea surface chlorophyll) are believed to significantly influence recruitment of skipjack tuna and can produce widely varying recruitment levels

between years. Druon et al. (2016) showed that there is significant correlation between the size of favourable feeding habitat, catch rates and total catches of skipjack in the Indian Ocean, and that SKJ populations respond rapidly to annual changes in the occurrence of productive surface fronts. Marsac (2023) discovered a high correlation between the annual recruitment deviations predicted by the assessment model and the sea surface chlorophyll (as a proxy for ocean productivity). The high recruitment anomaly estimated in 2022 appears to be supported by the strong positive phase of sea surface chlorophyll.

The model ensemble adopted for the previous assessment included an additional spatial dimension. The spatial partition could more effectively account for differential regional depletion and the absence of basin-scale tag mixing, thus reducing the potential bias inherent in the aggregated model. However, the extra complexity brought by the spatial structure necessitates greater data support, which the model most likely lacks (for instance, limited tag releases and recovery across area boundaries are not informative of movement). The ability of the model to estimate the relative level of biomass among regions is also weakened by the absence of information needed to correlate the various CPUE indicators among regions (Hoyle and Langley 2018). Given these issues, the spatially disaggregated model requires further development and was therefore not considered for the proposed model ensemble. The previous model ensemble also had a downweighting option for the tagging data, which accounted for some of the uncertainty associated with the tagging data. This option was based on the consideration that proper mixing of the tagged and untagged population might never occur at the basin scale. However, there is a wide concern over the accuracy of the PL index, which is very spatially constrained, and the PSLS index, which is based on fish aggregations and may experience hyperstability. With the range of model options explored, downweighting or removing the tagging data produced estimates of MSY values that seemed to be unrealistic (twice the highest historical skipjack catches).

Growth is an important source of uncertainty. As the change in mean size of a fished population relative to the unfished state is interpreted by the model as being linked to fishery-induced depletion, the lack of large fish in the catch, relative to a higher asymptotic length in the model would imply a higher level of fishing mortality and, hence a large fishery depletion effect. There is high degree of uncertainty in the growth estimates used for skipjack assessment. The L^∞ parameter estimated by Eveson et al. 2012 was about 70 cm, which was based on tagging data where only a few tags were recovered above 70 cm. An earlier study (Evenson 2011) fixed the L^∞ at 75 or 83 cm when estimating the growth curve, in recognition of the mode of large SKJ observed in the (poorly sampled) longline fishery. Based on the similar RTTO-IO data, Gartner et al. (2011) estimated L^∞ to be 76.9 cm (the study used Fabens's method as opposed to the LEP approach as in Eveson et al. 2012). A collation of growth parameter estimates from a vast array of regional studies for skipjack in the world's oceans shows an average/median L^∞ of 81 cm (Murua et al. 2017). Higher L^∞ values are currently used for skipjack assessment in the Atlantic (67, 76, and 87 cm, ICCAT 2009) and Pacific (74, and 86 cm. Jordan *et al.* 2012). Rapid-growing, individual skipjack with a fork length of 80 cm are common, while maximum fork length is thought to be about 110 cm (WWF 2015). Given above by having the option of estimating L^∞ within the model allowed some of the uncertainty associated with growth parameters to be incorporated into the assessment to a certain extent. The estimates of L^∞ range from 78-81 cm across the model ensemble.

Based on these preliminary results, the stock is considered not to be overfished and is not subject to overfishing in 2022. The high productivity and life history characteristics of skipjack tuna (fast growing, early maturation, and high fecundity) suggest that this species is resilient and not easily prone to overfishing (ISSF 2012). However, some of the early analysis of fishery trend based on indicators of PS fishery up until mid-2010s, including declining SKJ catches for purse seiners, declining percentages and catch rates of SKJ in FAD schools, decline of SKJ catch per FAD sets, reduced average weight of SKJ during this period, suggested symptoms of overfishing in the Western Indian Ocean (Marsac et al. 2017, Fonteneau 2014). The analysis of the correlation between the annual size of favourable feeding habitat and the catch rates and the total catches of skipjack using an ecological niche model agrees with the near full exploitation of skipjack in the IO since the 2000s and the subsequent decline in population productivity as regulated by habitat size (Druon, et al. 2016). The recent increase in PS FAD CPUE

associated with declining catch rate in the free schools could be a result of school fragmentation (Fonteneau and Marsac 2016), which hypothesized that the growing number of drifting FADs could have partitioned biomass from free schools. There could also be environmental changes or fluctuations (e.g., reduced feeding habitats) that resulted in a geographical contraction in SKJ populations and therefore higher fishing accessibility (Druon, et al. 2016).

8. ACKNOWLEDGMENTS

Thanks to the many people that contributed to the collection of this data historically, analysts involved in the CPUE standardization, and developers for providing the SS3 software.

9. REFERENCES

- Adam, M.S. 2010. Declining catches of skipjack in the Indian Ocean – observations from the Maldives. IOTC-2010-WPTT-09.
- Baidai, Y., Dupaix, A., Duparc, A., Dagorn, L., Deneubourg, J.L., Capello, M. 2023. Associative Behavior-Based abundance Index (ABBI) for western Indian Ocean skipjack tuna (*Katsuwonus pelamis*) obtained from echosounder buoys data. IOTC-2023-WPTT25(DP)-12.
- Chassot, E, Assan, C, Esparon, J., Tirant, A., Delgado d, Molina, A., Dewals, P., Augustin, E., Bodin, N. 2016. Length-weight relationships for tropical tunas caught with purse seine in the Indian Ocean: Update and lessons learned. IOTC-2016-WPDCS12-INF05.
- Chassot, E., Floch, P., Dewals, V., Fonteneau, R., Pianet. 2010. Statistics of the main purse seine fleets fishing in the Indian Ocean, 1981-2009. IOTC-2010-WPTT-13.
- Dammannagoda, S.T., Hurwood, D.A., Mather, P.B. 2011. Genetic analysis reveals two stocks of skipjack tuna (*Katsuwonus pelamis*) in the northwestern Indian Ocean. *Can. J. Fish. Aquat. Sci.* 68: 210-223.
- Delgado de Molina, A., Areso, J.J., Ariz, J. 2010. Statistics of the purse seine Spanish fleet in the Indian Ocean (1984-2009). IOTC-2010- WPTT-19.
- Druon, J.N., Chassot, E., Murua, H., Soto, M. 2016. Preferred feeding habitat of skipjack tuna in the eastern central Atlantic and western Indian Oceans: relations with carrying capacity and vulnerability to purse seine fishing. IOTC-2016-WPTT18-31.
- Eveson, J.P. 2011. Preliminary application of the Brownie-Petersen method to skipjack tag-recapture data. IOTC-2011-WPTT-13-31Rev_1
- Eveson, J.P., Million, J., Sardenne, F., Le Croizier, G. 2012. Updated Growth estimates for Skipjack, Yellowfin and Bigeye Tuna in the Indian Ocean using the most recent Tag-Recapture and Otolith data. IOTC-2012-WPTT-14-23Rev_1
- Fonteneau, A. 2014. On the movements and stock structure of skipjack (*Katsuwonus pelamis*) in the Indian ocean. IOTC-2014-WPTT16-36.
- Fu. 2017. Indian Ocean skipjack tuna stock assessment 1950-2016 (Stock synthesis). IOTC-2017-WPTT19-47.
- Fu. 2020. Preliminary Indian Ocean skipjack tuna stock assessment 1950-2019 (Stock synthesis). IOTC-2020-WPTT22-10.
- Fonteneau, A., Marsac, F. 2016. Fishery indicators suggest symptoms of overfishing for the Indian Ocean skipjack stock. IOTC-2016-WPTT18-INF02, 15p.

- Gaertner, D., Hallier, J.P., Dortel, E., Chassot, E., Fonteneau, A. 2011. An update of the Indian Ocean skipjack growth curve parameters with tagging data. Some new evidences on area-specific growth rates. IOTC-2011-WPTT13-INF14.
- Gaertner, D., Katara, I., Billet, N., Fonteneau, A., Lopez, J., Murua, H., Daniel, P. 2017. Workshop for the development of Skipjack indices of abundance for the EU tropical tuna purse seine fishery operating in the Indian Ocean. 17-21 July 2017. AZTI, Spain.
- Gaertner, D., Hallier, J.P. 2014. Tag shedding by tropical tunas in the Indian Ocean and other factors affecting the shedding rate. Fish. Res. (2014).
- Grande, M., Murua, H., Zudaire, I., Korta, M. 2010. Spawning activity and batch fecundity of skipjack, *Katsuwonus pelamis*, in the Western Indian Ocean. IOTC-2010-WPTT-47.
- Grande, M., Murua, H., Zudaire, I., Goni, N., & Bodin, N. (2014). Reproductive timing and reproductive capacity of the Skipjack Tuna (*Katsuwonus pelamis*) in the western Indian Ocean. Fisheries Research, 156, 14-22.
- Grewe, P.M., Wudianto, C.H., Proctor, M.S., Adam, A.R., Jauhary, K., Schafer, D., Itano, K., Evans, A., Killian, S., Foster, T., Gosselin, P., Feutry, J., Aulich, R., Gunasekera, M., Lansdell C.R. Davies. 2019. Population Structure and Connectivity of Tropical Tuna Species across the Indo Pacific Ocean Region. WCPFC-SC15-2019/SA-IP-15.
- Hallier, J.P., Million, J. 2009. The contribution of the regional tuna tagging project – Indian Ocean to IOTC stock assessment. IOTC-2010-WPTT-24.
- Hillary, R.M., Million, J., Anganuzzi, A., Areso, J.J. 2008a. Tag shedding and reporting rate estimates for Indian Ocean tuna using double-tagging and tag-seeding experiments. IOTC-2008-WPTDA-04.
- Hillary, R.M., Million, J., Anganuzzi, A., Areso, J.J. 2008b. Reporting rate analyses for recaptures from Seychelles port for yellowfin, bigeye and skipjack tuna. IOTC-2008-WPTT-18.
- Hoyle, S.D., Leroy, B.M., Nicol, S.J., Hampton, J. 2015. Covariates of release mortality and tag loss in large-scale tuna tagging experiments. Fisheries Research 163, 106-118.
- Hoyle, S.D., Langley, A. 2018. Indian Ocean tropical tuna regional scaling factors that allow for seasonality and cell areas. IOTC-2018-WPM09-13.
- IOTC 2016. Resolution 16/02. On Harvest Control Rules for skipjack tuna in the IOTC Area of Competence. IOTC Resolution 16/02.
- IOTC 2017. Report of the 19th Session of the IOTC Working Party on Tropical Tunas. Seychelles, 17–22 October 2017. IOTC–2017–WPTT19–R: 118 pp.
- IOTC 2020. Report of the 22nd Session of the IOTC Working Party on Tropical Tunas. Online, 22 - 24 June 2020. IOTC–2020–WPTT22(DP)–R: 35 pp
- IOTC 2023. Review of Indian ocean skipjack tuna statistical data. IOTC-2023-WPTT25(DP)-07.2_Rev1.
- ISSF 2011. Report of the 2011 ISSF stock assessment workshop. Technical Report ISSF Technical Report 2011-02, Rome, Italy, March 14-17, 2011.
- ISSF 2012. Stock Status Ratings, 2012: Status of the world fisheries for tuna. ISSF

Technical Report 2012-04B. International Seafood Sustainability Foundation, Washington, D.C., USA.

Itano, D. 2000. The reproductive biology of yellowfin tuna (*Thunnus albacares*) in Hawaiian waters and the western tropical Pacific Ocean: Project summary. JIMAR Contribution 00-328 SOEST 00-01.

Jauharee, A.R., Adam, M.S. 2009. Small Scale Tuna Tagging Project – Maldives 2007 Project Final Report - October 2009. Marine Research Centre, Malé 20-025, Republic of Maldives. Unpublished report, 17p.

ICCAT 2022. Report of the 2022 skipjack stock assessment meeting.
https://www.iccat.int/Documents/Meetings/Docs/2022/REPORTS/2022_SKJ_SA_ENG.pdf

Jordan, C.C., et al. 2022. Stock assessment of skipjack tuna in the western and central Pacific Ocean: 2022. WCPFC-SC18-2022/SA-WP-01 (REV5)

Kaplan, D.M., Grande, M., Alonso, M., Báez, J.C., Duparc, A., Imzilen, T., Floch, L., Santiago, J. 2023. Long time series CPUE standardization for skipjack tuna (*Katsuwonus pelamis*) of the EU purse-seine fishery on floating objects (FOB) in the Indian Ocean. IOTC-2023-WPTT25(DP)-INF05.

Kayama, S., Tanabe, T., Ogura, M., Okamoto, H. and Y. Watanabe. 2004. Daily age of skipjack tuna, *Katsuwonus pelamis* (Linnaeus), in the eastern Indian Ocean. IOTC-2004-WPTT-03.

Kiyofuji, H., Aoki, Y., Kinoshita, J., Ohashi, S., Fujioka, K. 2019. A conceptual model of skipjack tuna in the Western and Central Pacific Ocean (WCPO) for the spatial structure configuration. WCPFC-SC15-2019/SA-WP-11.

Kolody, D., Herrera, M., Million, J. 2011. Indian Ocean Skipjack Tuna Stock Assessment 1950-2009 (Stock Synthesis). IOTC-2011-WPTT13-31_Rev1.

Kolody, D., Eveson, J.P., Preece, A.L., Davies, C.R., Hillary, R.M. 2018. Recruitment in tuna RFMO stock assessment and management: A review of current approaches and challenges. Fisheries Research Volume 217, 217-234.

Maunder, M.N., Piner, K.R., 2015. Contemporary fisheries stock assessment: many issues still remain. ICES J. Mar. Sci. 72, 7–18.

McKechnie, S. Hampton, J., Pilling, G. M., Davies N. 2016. Stock assessment of skipjack tuna in the western and central Pacific Ocean. WCPFC-SC12-2016/SA-WP-04.

Marsac, F. 2023. Environmental signal in skipjack tuna recruitment in the Indian Ocean. IOTC-2023-WPTT25(DP)-09.

Mohamed, S. 2007. A bioeconomic analysis of Maldivian skipjack tuna fishery. M.Sc. thesis, University of Tromsø. 39 pp.

Marsac, F., Fonteneau, A., Lucas, J., Báez, J., Floch, L. 2017. Data-derived fishery and stocks status indicators for skipjack tuna in the Indian Ocean Floch. IOTC-2017-WPTT19-09.

Murua, H., Kitakado, T., Mosqueira, I., Adam, S., Merino, G., Fu, D., Bentley, N. 2017. Calculation of Skipjack Catch Limit for the Period 2018-2020 Using the Harvest Control Rule Adopted in Resolution 16/02. IOTC-2017-SC20-12 Rev_1.

Murua, H., Rodriguez-Marin, E., Neilson, J.D. et al. Fast versus slow growing tuna species: age,

growth, and implications for population dynamics and fisheries management. *Rev Fish Biol Fisheries* 27, 733–773 (2017). <https://doi.org/10.1007/s11160-017-9474-1>

Medley, P., Ahusan, M., Adam, M.S. 2023. Bayesian Skipjack and Yellowfin Tuna CPUE Standardisation Model for Maldives Pole and Line 1995-2022. IOTC-2023-WPTT25(DP)-13

Methot Jr, R.D., Wetzel, C.R. (2013) Stock synthesis: A biological and statistical framework for fish stock assessment and fishery management. *Fisheries Research*, 142(0): 86-99.

Methot Jr, R.D., Taylor, I.G., Doering, K. 2020. 2020. Stock Synthesis User Manual Version 3.30.15. U.S. Department of Commerce, NOAA Processed Report NMFS-NWFSC-PR-2020-05.

Nishikawa, Y., Honma, M., Ueyanagi, S., Kikawa, S. 1985. Average distribution of larvae of oceanic species of scombrid fishes, 1956–1981. *Far Seas Fisheries Research Laboratory, Shimizu. S Series 12. WPTT-04-06.*

Sharma, R., Herrera, M., Million, J. 2012. Indian Ocean Skipjack Tuna Stock Assessment 1950-2011 (Stock Synthesis). IOTC–2012–WPTT14–29 Rev–1.

Sharma, R., Herrera, M., Million, J. 2014. Indian Ocean Skipjack Tuna Stock Assessment 1950-2013 (Stock Synthesis). IOTC–2014–WPTT16–43 Rev_3.

Wujdi, A., Setyadji, Bram., Nugroho, S. C. 2017. Preliminary stock structure study of skipjack tuna (*Katsuwonus pelamis*) from south java using otolith shape analysis. IOTC-2017-WPTT19-xx.

Walter, J., Winker, H., 2019. Projections to create Kobe 2 Strategy Matrices using the multivariate log-normal approximation for Atlantic yellowfin tuna. ICCAT-SCRS/2019/145 1–12.

Winker, H., Walter, J., Cardinale, M., Fu, D. 2019. A multivariate lognormal Monte-Carlo approach for estimating structural uncertainty about the stock status and future projections for Indian Ocean Yellowfin tuna. IOTC–2019–WPTT21–51.

WWF 2015. WWF Fact Sheet: skipjack tuna (*Katsuwonus pelamis*).

Vincent, M. T., Pilling, G.M., J Hampton, J. 2019. Stock assessment of skipjack tuna in the western and central Pacific Ocean. WCPFC-SC15-2019/SA-WP-05-Rev2.

Zudaire, I. 2022. Preliminary estimates of sex ratio, spawning season, batch fecundity and length at maturity for Indian Ocean skipjack tuna. IOTC-2021-SC24-INF02

APPENDIX A: SELECTED RESULTS FROM THE SENSIVITY MODELS

Table B1. Maximum Posterior Density (MPD) estimates of the main stock status indicators from the sensitivity model options.

	SB_0	SB_{MSY}	SB_{2022}	SB_{2022}/SB_0	SB_{2022}/SB_{MSY}	F_{2022}/F_{MSY}	$F_{40\%SB}$	F_{MSY}	MSY	<i>Max. grad</i> <i>(0.0001)</i>
<i>basic</i>	1 734 090	419 342	1 257 130	0.72	3.00	0.41	0.62	1.06	540 824	0.0002
<i>PL</i>	1 826 990	437 787	1 393 910	0.76	3.18	0.38	0.61	1.05	560 600	0.00009
<i>PSLS</i>	2 121 290	505 021	1 377 500	0.65	2.73	0.39	0.60	1.04	641 512	0.00008
<i>behaviour</i>	2 016 190	479 074	971 370	0.48	2.03	0.56	0.60	1.05	609 441	0.0003
<i>Tag01</i>	2 061 790	497 977	1 654 170	0.80	3.32	0.32	0.61	1.05	633 962	0.0003
<i>tagEx</i>	2 152 650	518 931	1 776 190	0.83	3.42	0.30	0.60	1.05	659 106	0.0008
<i>Linf</i>	2 402 830	581 151	994 121	0.41	1.71	0.79	0.44	0.79	477 536	0.0027
<i>seas</i>	2 113 790	508 901	1 728 960	0.82	3.40	0.31	0.60	1.05	647 316	0.0003
<i>st1980</i>	1 722 740	420 634	1 201 220	0.70	2.86	0.43	0.62	1.07	542 513	0.002

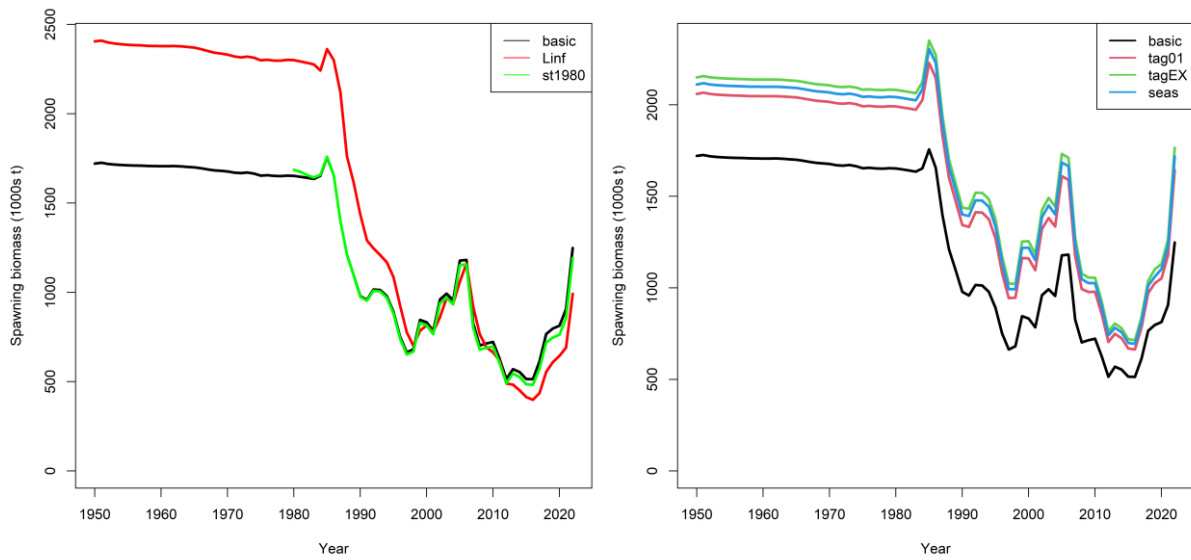


Figure A1: A comparison of estimated spawning biomass from sensitivity models (see Table 4 for a description of sensitivity).

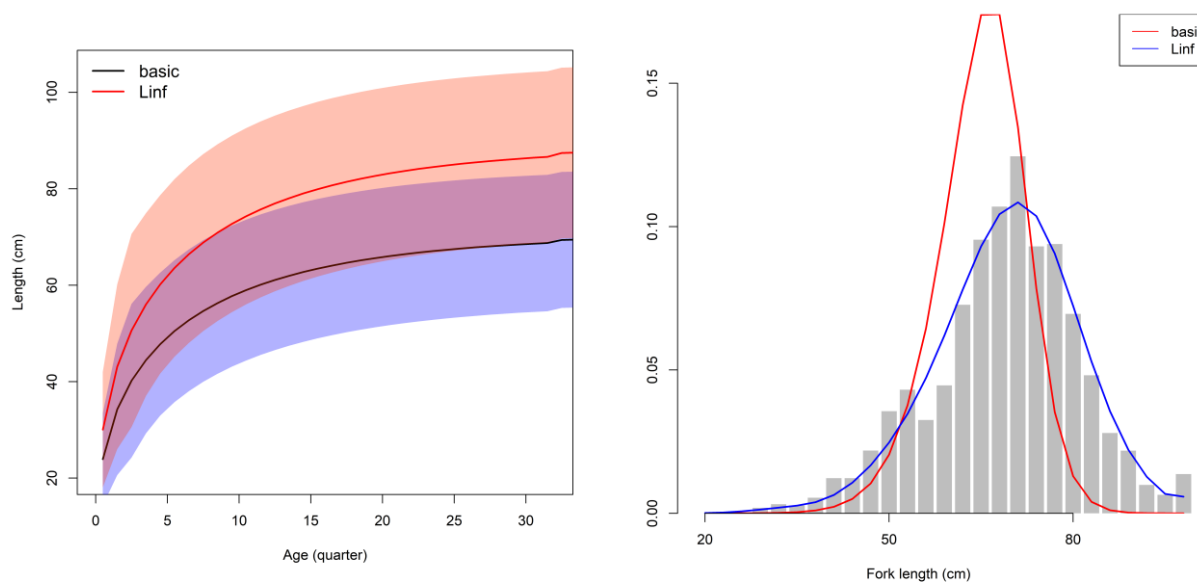


Figure A2: A comparison of estimated growth (L^∞) *Linf* and the fixed growth ($L^\infty = 70\text{ cm}$) (left), and fits to the longline length compositions (aggregated) between model *Linf* and the *basic* model.

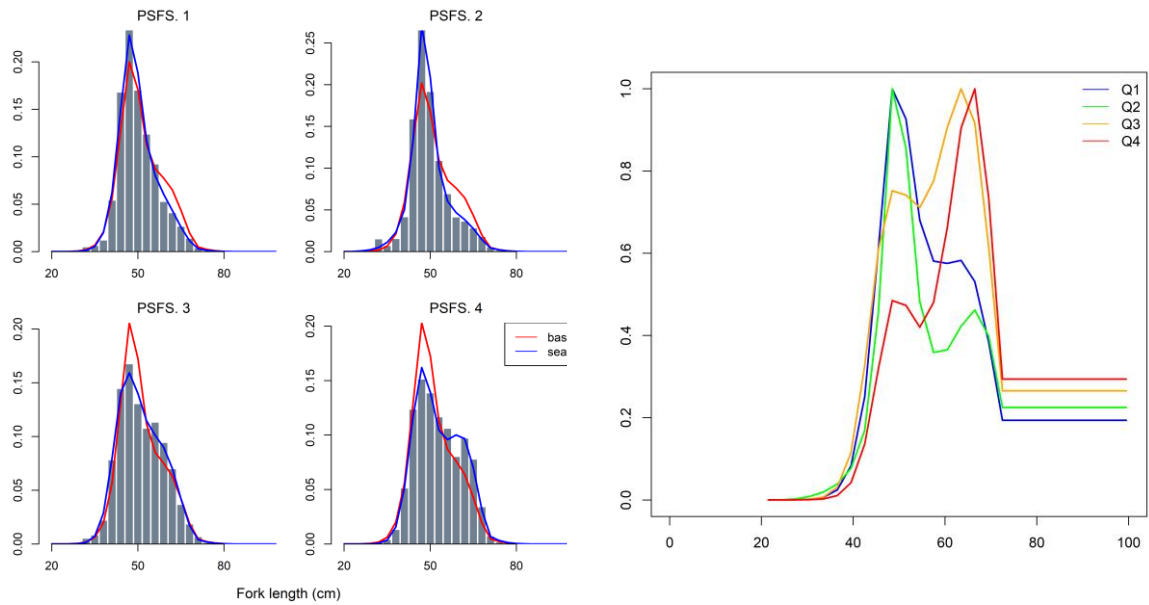


Figure A3: A comparison of fits to the PSFS length compositions (aggregated for each quarter) between model *seas* and the basic model (left), and estimated selectivity for each quarter for model *seas* (right).